NIST Special Publication 250-98

LIQUID FLOW METER CALIBRATIONS WITH NIST's 15 kg/s WATER FLOW STANDARD

Jodie G. Pope
Aaron N. Johnson
B. James Filla
Vern E. Bean
Michael R. Moldover
Joey T. Boyd
Christopher J. Crowley
Iosif I. Shinder
Keith A. Gillis
John D. Wright

This publication is available free of charge from:
https://doi.org/10.6028/NIST.SP.250-98

National Institute of Standards and Technology
U.S. Department of Commerce

NIST Special Publication 250-98

LIQUID FLOW METER CALIBRATIONS WITH NIST's 15 kg/s WATER FLOW STANDARD

Jodie G. Pope
Aaron N. Johnson
B. James Filla
Vern E. Bean
Michael R. Moldover
Joey T. Boyd
Christopher J. Crowley
Iosif I. Shinder
Keith A. Gillis
John D. Wright
Fluid Metrology Group
Sensor Science Division
National Institute of Standards and Technology, Gaithersburg, MD

Office of Information Management
Innovations and Solutions Division
National Institute of Standards and Technology, Boulder, CO

This publication is available free of charge from:
https://doi.org/10.6028/NIST.SP.250-98

June 2021

U.S. Department of Commerce
Gina M. Raimondo, Secretary

National Institute of Standards and Technology
James K. Olthoff, Performing the Non-Exclusive Functions and Duties of the Under Secretary of Commerce for Standards and Technology & Director, National Institute of Standards and Technology

National Institute of Standards and Technology Special Publication 250-98
Natl. Inst. Stand. Technol. Spec. Publ. 250-98, 44 pages (June 2021)
CODEN: NSPUE2

This publication is available free of charge from:
https://doi.org/10.6028/NIST.SP.250-98

LIQUID FLOW METER CALIBRATIONS WITH NIST's 15 kg/s WATER FLOW STANDARD

NIST Special Publication 250-98

Jodie G. Pope, Aaron N. Johnson, B. James Filla, Vern E. Bean, Michael R. Moldover, Joey T. Boyd, Christopher J. Crowley, Iosif I. Shinder, Keith Gillis, and John D. Wright

June 2021

Contents

Abstract

We describe the 15 kg/s water flow calibration standard operated by the Fluid Metrology Group of the National Institute of Standards and Technology (NIST) to calibrate liquid flow meters for customers. The 15 kg/s standard is a dynamic, gravimetric, liquid flow standard (LFS) that determines flow by measuring the rate of change of the mass of water accumulating in a collection tank. The LFS is a fully automated system that uses two proportional–integral–derivative control loops to achieve water flows near ambient temperature with a mass flow stability that is the smaller of 0.001 % of the mass flow set point or 0.1 kg/s. The expanded uncertainty of the LFS is 0.022 % for mass flow and 0.023 % for volume flow for the flow range 0.22 kg/s to 15 kg/s. (Unless stated otherwise, all uncertainties have a 95 % confidence level.) When the LFS is used to calibrate a customer's meter, the uncertainty of the meter factor is increased by the irreproducibility of the meter under test (MUT). The most reproducible meters tested by NIST have meter-factor uncertainties of 0.035 % and 0.036 % for mass flow and volume flow, respectively. Below, we derive the equation for calculating flow at the meter under test, analyze the uncertainty of the flow standard, give supporting data, and provide a sample calibration report. This document also describes the procedures that customers must follow to submit their flow meters to NIST for calibration.

Key Words: Calibration, Dynamic Gravimetric Flow Standard, Flow Meter, Uncertainty, Liquid Flow Standard

1.0 Introduction

Flow measurement units are derived from the SI (International System of Units) base units. Therefore, the paths taken to realize flow measurement standards vary and depend upon, for example, the properties of the fluid(s) to be measured. NIST's flow standards are based on fundamental measurements such as mass, length, time, and temperature. Typically, these standards account for the transfer of a known mass or volume of fluid during a measured time interval under approximately steady state conditions of flow, pressure, and temperature at the meter under test (MUT). Such standards are known as "primary flow standards"; by definition [1], they determine flow with quantified uncertainties, while being traceable to fundamental units of mass, time, *etc.*, and not by calibration against another flow device. This document describes NIST's 15 kg/s primary liquid flow standard (LFS), which spans the flow range of 0.22 kg/s to 15 kg/s with expanded uncertainty of 0.022 % for mass flow and 0.030 % for volume flow (with a 95 % confidence level)[i] in the test section where the MUT is installed. When the LFS calibrates a MUT, the uncertainty of the meter factor is increased by the irreproducibility of the MUT and, for pulse-generating meters, the uncertainty of the measured frequency. Based on NIST's experience with high-quality MUTs, the expanded uncertainty for the meter factor is equal to or greater than 0.035 % for mass flow and 0.036 % for volume flow[ii]. The uncertainty analysis for the 15 kg/s LFS has been validated by comparisons to NIST's older primary liquid flow standards, including a static gravimetric standard and a diverter-based flow standard.

The 15 kg/s LFS is a dynamic gravimetric water flow standard; the water flowing through the MUT is collected in a large tank, and the flow is determined from the rate of change of the weight of the collection tank. [2]. The system is termed *dynamic* gravimetric because the mass measurements are made *while the tank is filling* and the mass of collected water is changing. In contrast, the weight of the

[i] Standard uncertainty with coverage factor $k = 1$, refers to 68 % confidence level and expanded uncertainty with $k = 2$ refers to 95 % confidence level. For expanded uncertainty $k \approx 2$, however, effective degrees of freedom and the associated t-value must be considered for the true k value corresponding to 95 % confidence level.

[ii] The expanded uncertainty in the meter factor is larger than that of the mass flow or the volume flow because it includes 1) the standard deviation of the mean of ten repeated measurements of the MUT (approximately 0.01 % for high-quality MUTs) and 2) the ability to measure the pulse output of the MUT (0.009 %). The given values will be different for a customer meter because the repeatability may differ from NIST's device.

collection tank of a *static* gravimetric standard is measured when flow is neither entering nor exiting the tank; hence its weight is unchanging or static.
Figure 1 is a schematic diagram of the dynamic standard. The standard consists of a water source (the reservoir tank), a variable speed pump, a straight test section that contains a Coriolis flow meter, temperature and pressure transducers, a collection tank resting on a weigh scale, and a data acquisition system that records the time-stamped weigh scale readings and the environmental variables and controls the valves and pump. The Coriolis meter serves as a check standard to detect problems in the flow measurements made by the primary standard. The Coriolis meter also provides input to a proportional-integral-derivative (PID) control loop that continuously adjusts the position of a butterfly valve to maintain the desired steady mass flow. A second PID control loop maintains constant pressure in the test section, where the MUT is installed, by continuously adjusting the pump speed via a variable speed drive based on input from the downstream pressure sensor. The flow is computed by weighing the collection tank and correcting for air buoyancy approximately 5 times every second while it is filled by a steady water flow. The output of the MUT is measured every time the tank is weighed. All of the quantities measured in connection with the calibration standards (mass, temperature, *etc*.) are traceable to established United States national standards.

NIST calibrates liquid flow meters to provide traceability for flow meter manufacturers, secondary flow calibration laboratories, and flow meter users. We calibrate a customer's flow meter and deliver a calibration report that documents the calibration procedure, the calibration results, and their uncertainty on a fee-for-service basis. Often, the calibrated flow meter is used as a transfer standard to compare the customer's primary standards to the NIST primary standards so that the customer can establish traceability, validate their uncertainty analysis, and demonstrate proficiency. Customers with no primary standards use their NIST-calibrated flow meters as working standards or reference standards

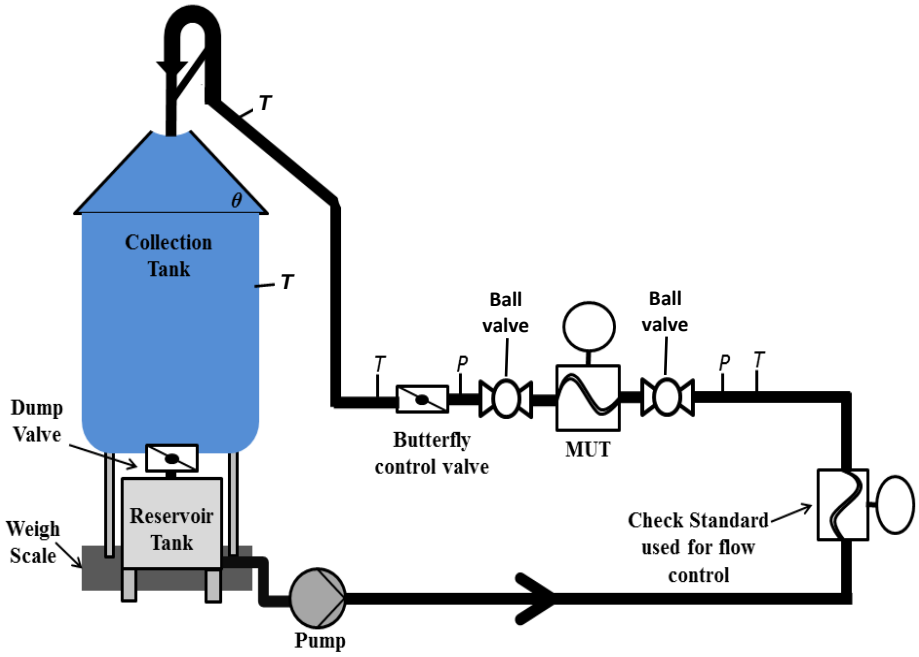

Fig. 1. Schematic of the 15 kg/s LFS. Initially, flow is pumped around the loop, through the MUT located in the test section and the collection tank with the dump valve open. To collect calibration data, the dump valve is closed and time-stamped readings from the weigh scale are recorded with a data acquisition system. The locations of pressure and temperature transducers are indicated by "*P*" and "*T*".

in their laboratory to calibrate other flow meters. The Report of Calibration is the property of the customer. NIST treats the results of calibrations as proprietary information belonging to the customer.

Often, NIST performs proficiency testing for customers who maintain their own primary standards. For these tests, a transfer standard flow meter is calibrated by the customer at the customer's facility using their flow reference and subsequently at NIST using the 15 kg/s LFS. The results of this proficiency test document the difference in the meter factor determined by NIST and by the customer relative to the combined uncertainty of the calibrations at both laboratories. These tests validate the claimed uncertainties of the customer's primary standards and are generally required by accreditation bodies to demonstrate technical proficiency and to assure the quality of test and calibration results associated with the customer's primary standard [3]. Since proficiency tests serve as an independent verification of a customer's calibration capabilities, the customer must provide NIST with their calibration results (*i.e*., meter factor and corresponding uncertainty) before NIST shares the results and compiles the report. The meter factor uncertainty submitted to NIST should include the uncertainty attributed to the calibration process as well as the relevant uncertainty contribution from their flow standard. We include a detailed uncertainty analysis in this manuscript as an example of how to perform an uncertainty analysis and to support our claimed 0.022 % expanded uncertainty for NIST's 15 kg/s LFS. [4]

2.0 Description of Measurement Services

To find the most current information regarding NIST's calibration services, calibration fees, technical contacts, and flow meter submittal procedures, customers should consult the web address https://shop.nist.gov/ and search for "flow meter".

Typically, NIST's 15 kg/s LFS is used to calibrate pulse generating flow meters (*e.g*., turbine meters, positive displacement meters, Coriolis meters), but it can be used to calibrate other meter types. The liquid used for calibrations is tap water. Although NIST does not control the water's temperature during the calibration, it changes less than 0.05 K during a calibration. NIST maintains a variety of fittings, including Swagelok[iii], A/N 37-degree flare, sanitary, flange, and national pipe thread (NPT), that are used to install customer flow meters into the LFS. Other fittings can be accommodated; however, piping connections should be discussed with NIST before sending a flow meter for calibration.

Both upstream and downstream from the MUT, the 15 kg/s LFS has runs of straight pipe that are 1.5 m long with an inside diameter of 5 cm (*i.e*., 30 pipe diameters of straight run). The upstream run provides a well-developed turbulent profile at the MUT. Customers may submit flow conditioners with their meters if they would like them installed upstream of the MUT during the calibration.

NIST accepts meters for calibration with the LFS if the flow range and piping connections are suitable and if the precision of the customer's meter is commensurate with the uncertainty of the LFS. Meter types with calibration instability significantly larger than the LFS's uncertainty are generally not calibrated with NIST's standards because such meters can be calibrated with acceptable uncertainties at a lower cost by commercial laboratories.

Normally, NIST's Fluid Metrology Group calibrates a customer's flow meter at five flows: 10 %, 30 %, 50 %, 75 %, and 100 % of its full scale. At each of these flows, five consecutive flow measurements are made on two separate occasions, typically within 48 hours. Therefore, the final data set consists of ten flow measurements made at five flow set points, *i.e*., 50 flow measurements. The sets of five measurements can be used to assess repeatability, while the sets of ten can be used to assess

[iii] Certain commercial equipment, instruments, or materials are identified in this paper to foster understanding. Such identification does not imply recommendation or endorsement by the National Institute of Standards and Technology, nor does it imply that the materials or equipment identified are necessarily the best available for the purpose.

reproducibility [1]. For an example, see the sample calibration report in Appendix A of this document. Variations of the number of flow set points, the spacing of the set points, and the number of repeated measurements can be discussed with the NIST technical contacts. However, for data quality assurance, NIST rarely conducts calibrations involving fewer than three flow set points and two sets of three flow measurements at each set point.

When possible, the Fluid Metrology Group, tabulates calibration results in a dimensionless format that considers the physical model for the flow meter type. This dimensionless approach facilitates accurate flow measurements, even when the conditions of usage (*e.g.*, liquid type, temperature) differ from the conditions during calibration. Hence, for turbine meters (and other pulse generating volume flow meters), the calibration report will tabulate Strouhal number *versus* Roshko number [5, 6]. For a mass flow meter (*e.g.*, a Coriolis meter), the tabulated calibration factor is the ratio of the mass flow indicated by the LFS to the mass flow indicated by the MUT.

To provide traceable flow calibrations and to calculate the uncertainty of the flow meter calibration factor, NIST must know the uncertainty of its standards as well as the uncertainty of the instruments associated with the MUT (normally, frequency and temperature instruments). Usually, NIST-owned instruments are used during calibrations of the MUT because these instruments have established uncertainties based on calibration records maintained in NIST's Quality System: https://www.nist.gov/nist-quality-system Such information is often not available for customer-supplied instruments. The customer's instruments can be used for a calibration or a Special Test if specific arrangements are first made with NIST's technical contact. Calibration of a customer's ancillary instruments is not part of the calibration procedures described herein and, if requested, requires separate arrangements.

3.0 Procedures for Submitting a Flow Meter for Calibration

The Fluid Metrology Group follows the NIST calibration policies that are posted on the NIST web pages. More specific information about the flow calibration service, including the technical contacts in the Fluid Metrology Group, fee estimates, and turnaround times, can be found at: https://shop.nist.gov/ using the search term "flow meter".

4.0 Description of the Liquid Flow Standard

The dynamic gravimetric method used by the 15 kg/s LFS is well documented and is accepted as a low uncertainty means of calibrating liquid flow meters while avoiding the expense and complexity of either a flow diverter (generally used during static weighing methods) or the mechanical complexity of reciprocating provers [7, 8, 9]. The 15 kg/s LFS described here does not resemble NIST's less-accurate, previously described, dynamic flow standards that used a collection tank supported by a beam balance. [10]

As shown in Fig. 1, the 15 kg/s LFS is a fully-automated, flow loop that comprises three major subsystems: 1) a flow generation and control system consisting of a variable speed pump, reservoir tank, Coriolis flow meter (used as check standard and for flow control), butterfly valve, and data acquisition system with two digital PID controllers, 2) a dynamic weighing system composed of a collection tank and weigh scale that makes SI-traceable mass flow measurements, and 3) a test section where a customer's MUT is installed and calibrated. The test section accommodates MUTs with pipe diameters ranging from 1.25 cm to 5 cm.

Figure 2 is a photograph of the 15 kg/s LFS. We list the nominal specifications of the LFS in Table 1. The standard uses tap water as the working fluid. The water is stored at ambient pressure and is assumed to be saturated with dissolved air. (Dissolved air reduces water's density by less than 0.00021% at

25 °C. [11]) The weigh scale readings are recorded at 0.21 s intervals while the flow accumulates in the collection tank. As shown by Shinder and Moldover, the slope of the buoyancy-corrected weight measurements over time equals the mass flow if the mass flow is steady [7]. Custom-designed software written in National Instruments' LabVIEW[iii] environment operates the mechanical components of the LFS and acquires and stores calibration data. Calibrations are normally performed at ambient temperatures with water pressures no less than 140 kPa in the test section to avoid cavitation. Optionally, a thermostatted chamber can be used to control the environmental temperature surrounding the MUT at temperatures between 10 °C and 50 °C.

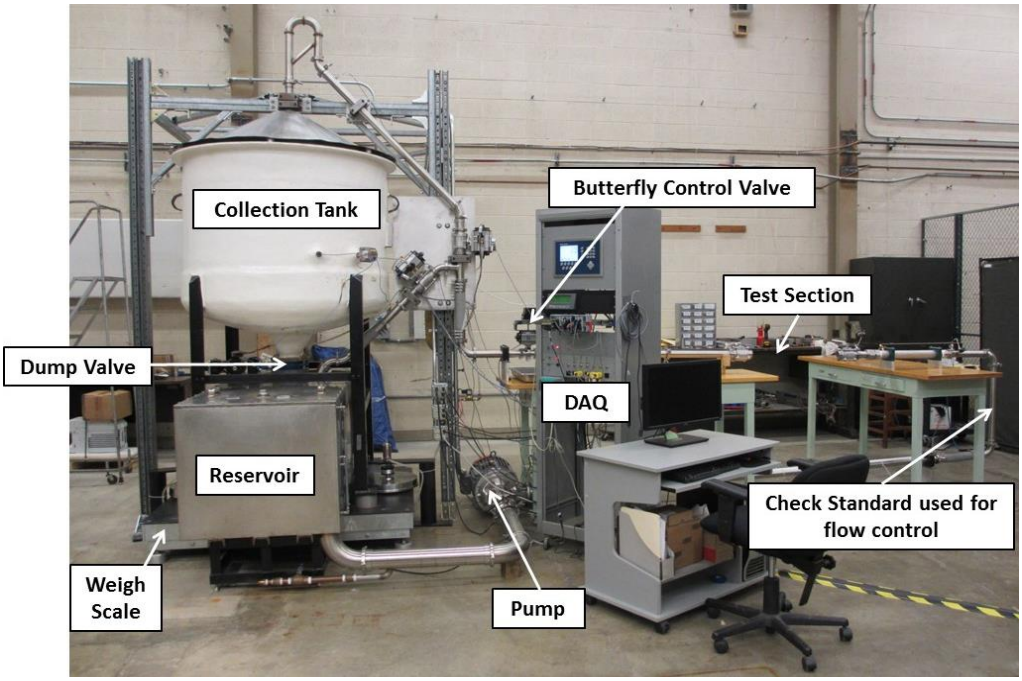

Fig. 2. The 15 kg/s Liquid Flow Standard. DAQ is the data acquisition system.

Table 1. Nominal Specifications of the 15 kg/s LFS

Test fluid	Water
Flow range	0.22 kg/s to 15 kg/s
Water Temperature [a]	20 °C to 25 °C
Pressure	140 kPa to 550 kPa
Volume of collection tank	0.90 m³
Volume of reservoir tank	1.1 m³
Diameter of piping	0.051 m
Total length of test section	3.3 m
Volume between MUT and collection tank	0.01 m³
Collection time	15 s to 3000 s

[a] Calibrations are performed with the fluid at the ambient temperature.

The 15 kg/s LFS was constructed in NIST's Fluid Mechanics Building. Upon completion, we calibrated the weigh scale and the time, pressure, and temperature instruments, thereby making the system directly traceable to NIST standards. We analyzed the uncertainty of these standards, and the results are documented below.

4.1 Flow generation, control, and stabilization

The 15 kg/s LFS generates and maintains a steady flow and pressure at each set point using a variable-speed pump, a butterfly valve, a Coriolis flow meter, and two PID controllers. The pump circulates the water and pressurizes the test section. One PID controller adjusts the butterfly valve to maintain constant flow through the Coriolis check meter at the set point specified in the LabVIEW[iii] program. The second PID controller adjusts the pump speed to keep the pressure constant. The flow is considered steady when two conditions are satisfied: 1) during an interval of 60 s, the absolute values of the first and second time-derivatives of the flow through the Coriolis meter are less than 0.0001 kg/s^2 and 0.01 kg/s^3, respectively, and 2) the measured flow is within the larger of ± 0.001 % or ± 0.1 kg/s of the set point.

A calibration cycle starts with a flow stabilization period during which the dump valve beneath the collection tank is open and the collection tank is not weighed. Water pumped from the reservoir tank flows through the check-standard Coriolis meter, the MUT, and finally through the collection tank before it returns to the reservoir. The dump valve closes to start a collection. Flow accumulates in the collection tank for 15 s to 200 s, depending on the flow. At the lowest flow (0.22 kg/s), the tank can collect liquid for up to 3000 s; however, such a large collection time and mass of water are not necessary to obtain acceptable uncertainty. Therefore, the operator saves time by reducing the collection time to 200 s, the minimum needed to collect at least 44 kg. Collections of 44 kg or more reduce to acceptable values the uncertainty contributions from the weigh scale's calibration and resolution. Following each collection interval, the dump valve opens to drain the collection tank into the reservoir, thereby preparing for the next flow measurement. Therefore, the collection tank is either filling or draining throughout a calibration cycle.

4.2 Dynamic weighing system

During a flow calibration, water is either continuously filling or continuously draining from the collection tank, depending on the position of the dump valve. The collection tank's drain hole is 10 cm in diameter and is opened and closed by the dump valve (Figs. 1 and 2). The collection tank drains directly into the reservoir tank, which is supported by the floor and not in contact with the weigh scale. The only part of the LFS in contact with the weigh scale is the collection tank and its removable cap. (See Figs 3. and 4). The cap prevents water from splashing out of the collection tank.

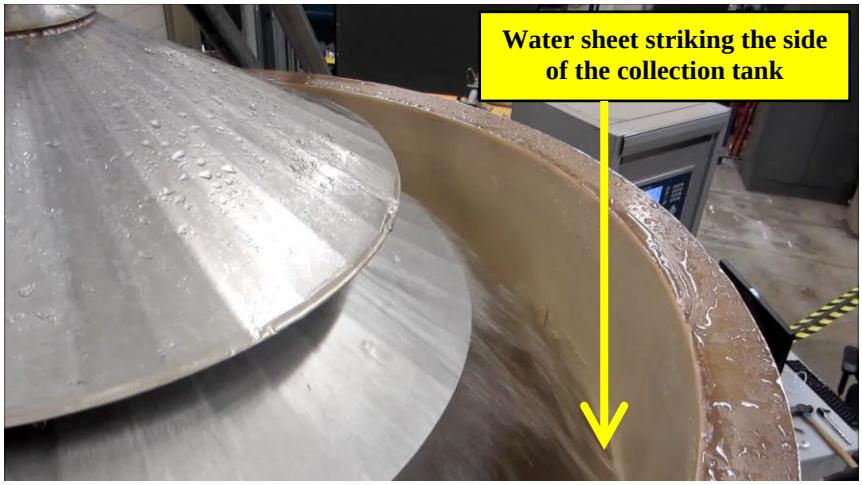

Fig. 3. Photograph of the two cones above the collection tank with the cap removed. The incoming water flows between the cones forming a sheet that strikes the vertical side of the collection tank. The flow shown is 10 kg/s. During normal use, the cap (identified in Fig. 4, below) rests on the collection tank without touching either cone. Thus, the cap is weighed; however, the cones are not weighed.

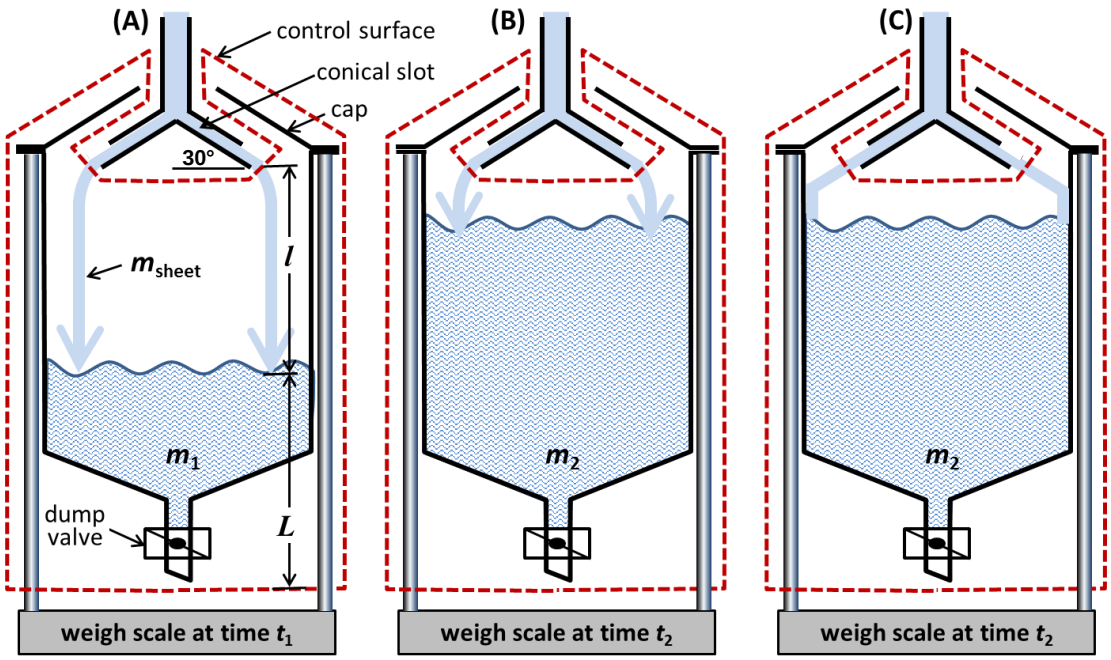

Fig. 4. The red dashed curve is the control surface for the momentum balance Eq. (6). The angle between the conical slot and the horizon is 30°. (A) water level at time t_1. (B) Higher water level at a later time t_2. (C) High flow situation in which the water sheet exiting the conical slot strikes the inside wall of the collection tank.

To obtain low-noise dynamic weighings, the water flow between the butterfly valve and the collection tank must be as steady as the water flow through the MUT. To achieve such a steady flow, the pipe leading from the butterfly valve to the collection tank has a goose neck that terminates in two concentric cones that lie beneath the tank's cap. Both cones are supported by the inlet pipe and neither cone is in contact with the tank nor its cover. The water flowing in the channel between the upper and lower cones forms an expanding, conical sheet that may strike the vertical side of the cylindrical collection tank (Fig. 3). Because the conical water sheet is concentric with the collection tank, flow-dependent, horizontal forces on the collection tank are sufficiently balanced and do not affect the weigh scale.

We thank Ron Benson for recommending the conical inlet scheme to us [12]. The conical inlet scheme avoided a flow instability that we observed while using an earlier dynamic flow standard. The inlet pipe of the earlier standard terminated with a "fishtail" above the collection vessel [7]. For flows near 20 kg/s, the flow exiting the fishtail randomly oscillated between two patterns: one that filled the fishtail completely, and one that underfilled the fishtail. The irregular oscillations between flow patterns generated excessive noise (Figs. 6 and 9 in Ref. [7]) in the apparent weight of the collection tank.

The weigh scale has a 1.2 m x 1.5 m platform with a 1500 kg capacity and 10 g resolution. The data acquisition system reads the scale output at intervals of 0.209718 s, as determined by the scale's internal 24 MHz clock. The stability of the 24 MHz clock was verified by multiple long-term timing tests (Section 8.2). The clock is checked before each customer calibration to ensure that it has not changed. Measurements from the flow meters and temperature and pressure sensors are also recorded every 0.21 s, as determined by the scale's clock. Measurements from an environmental monitor are recorded every 0.46 s.

4.3 Test section

The test section is a straight, stainless-steel pipe, 3.3 m long with a 5 cm diameter. During flow calibrations the MUT is installed at least 1.5 m downstream of a straight pipe run. If the straight run is considered inadequate to assure a fully developed turbulent flow, a flow conditioner can be installed near the inlet of the test section. We measure temperature and pressure upstream and downstream of the MUT. Because, the water temperature is not controlled, it increases by as much as 0.05 K during a flow measurement because of heating from the pump. The pressure in the test section is kept sufficiently high to avoid cavitation. The operator detects cavitation by listening through a stethoscope applied to the pipe wall near the MUT. The maximum pressure is limited by the pump to 552 kPa. During a collection, the pressure in the test section is controlled within 5 kPa; however, it varies with the flow and the size of the MUT. In general, the pressure increases with larger flows and smaller flow meters. Between the beginning and the end of a collection, the mass of water in the volume between the MUT and the pipe leading to the collection tank (Fig. 2) changes as the temperature and pressure changes. This "mass storage" effect is negligible: its uncertainty is discussed in Section 5.1. When calibrating a MUT that measures volume flow, we draw a sample of water from the collection tank and measure its density using a vibrating tube densimeter.

5.0 Flow Measurement Principle of Dynamic Weighing

Flow determinations are based on the rate of change of the mass of water in the collection tank, as deduced from repeated measurements of the tank's buoyancy-corrected weight. The average mass flow $\langle \dot{m} \rangle_{t1,t2}$ between times t_1 and t_2 is:

$$\langle \dot{m} \rangle_{t1,t2} = \left(\frac{m_2 - m_1}{t_2 - t_1} \right) = \frac{1}{g\left(1 - \rho_{\text{air}} / \rho_{\text{water}}\right)} \left(\frac{W_2 - W_1}{t_2 - t_1} \right) \quad , \tag{1}$$

where, $W_2 - W_1$ is the change in the reading of the weigh scale during the time interval $t_2 - t_1$. We recall that $W/(1 - \rho_{\text{air}}/\rho_{\text{water}})$ is a buoyancy corrected weight, g is the acceleration due to gravity, ρ_{air} is the air density, and ρ_{water} is the density of the water in the collection tank. (Appendix C defines the nomenclature used in this document.)

In the limit of infinitesimal time steps between weigh scale readings, Eq. (1) becomes the differential equation:

$$\lim_{t2-t1 \to 0} \langle \dot{m} \rangle_{t1,t2} = \dot{m}_{\text{scale}} = \frac{dm}{dt}, \tag{2}$$

where the subscript "scale" has been added to the mass flow to denote that it is determined from the buoyancy-corrected readings of the weigh scale.

We derive Eq. (2) using the Reynolds transport theorem [13, 14], which has the form:

$$\frac{d\Theta}{dt} = \frac{d}{dt} \int_{\text{CV}} \rho\theta \, d\mathcal{V} + \int_{\text{CS}} \rho\theta \vec{v}_{\text{r}} \cdot \hat{n} \, d\mathcal{S}, \tag{3}$$

where Θ is an extensive scalar quantity, and $\theta = \Theta / m$ is the intensive quantity (per unit mass) associated with Θ. The first term in Eq. (3) contains a volume integral with volume element $d\mathcal{V}$ over the control volume (CV), and the second term contains a surface integral with surface area element $d\mathcal{S}$ over the control surface (CS) that bounds CV. In Eq. (3) and following equations, ρ is the mass density at $\vec{r}$,

$\vec{v}_r$ is the velocity of the fluid at the CS relative to the CS, and $\hat{n}$ is the outward pointing normal unit vector at the CS. We choose the CS [dashed curve in Fig. 4(A)] to include the entire collection tank (including its cap but excluding the inlet cones) and to cut perpendicularly through the flowing liquid sheet exiting the conical slot. For this CS, the surface integral in Eq. (5) below is independent of the complicated flows and forces inside the CV. For Fig. 4, we choose $\Theta \equiv m$, where m is the mass of substance in the CV, and the intensive quantity becomes simply $\theta = 1$. Then, Eq. (3) becomes the conservation of mass:

$$0 = \frac{d}{dt}\left[m_{\text{tank}} + \int_{\text{CV}} \rho_{\text{fluid}}(\vec{r})\, d\mathcal{V} \right] + \int_{\text{CS}} \rho_{\text{fluid}} \vec{v}_r \cdot \hat{n}\, d\mathcal{S} = \dot{m}_{\text{water}} - \rho_{\text{water}} \left\langle v_0 A_{\text{sheet}} \right\rangle, \tag{4}$$

where m_{tank} is the mass of the empty tank, A_{sheet} is the area of the falling, approximately annular water sheet where it penetrates the CS, and $\langle v_0 A_{\text{sheet}} \rangle$ is the volume flow of water into the CV averaged over the circumference of the sheet. The surface term is negative because the normal vector $\hat{n}$ points out of the CV. Therefore, $\dot{m}_{\text{water}} = \rho_{\text{water}} \left\langle v_0 A_{\text{sheet}} \right\rangle$.

In Fig. 4(A), we are interested in the weigh scale readings as a function of the mass of water in the weigh tank and of the rate at which the water enters the tank. Therefore, we apply the Reynolds transport theorem to the same CV:

$$\sum \vec{F} \quad = \quad \frac{d}{dt} \iiint_{\text{CV}} \rho \vec{v}\, d\mathcal{V} \quad + \quad \iint_{\text{CS}} \rho \vec{v} \left(\vec{v}_r \cdot \hat{n} \right) d\mathcal{S} \tag{5}$$

$$\begin{bmatrix} \text{sum of all} \\ \text{external forces} \\ \text{acting on CV} \end{bmatrix} = \begin{bmatrix} \text{time rate of change} \\ \text{of linear momentum} \\ \text{of the contents in CV} \end{bmatrix} + \begin{bmatrix} \text{net flow of linear} \\ \text{momentum out of CS.} \\ \hat{n} \text{ points outward} \end{bmatrix}$$

The external forces include the body forces that act on the CV and surface forces, including normal and shear stresses, that act on the CS. We make a key assumption: the flow through the CS is steady; that is, the flow is independent of time. However, we do not assume that the flows in the conical slot and in the collection tank are axisymmetric. In Eq. (5), $\vec{v}_r$ is the velocity of the fluid at the CS surface relative to the CS. The control surface in Fig. 4 is stationary, therefore $\vec{v}_r = \vec{v}_0$. The momentum flow $\vec{\mathcal{P}}$ through the control surface is:

$$d\vec{\mathcal{P}} = \rho \vec{v}_0 \left(\vec{v}_0 \cdot \hat{n} \right) dS\,. \tag{6}$$

We apply the Reynolds transport theorem to the vertical-component (z-component) of the momentum:

$$-F_{\text{grav}} + F_{\text{Nscale}} = -\frac{d}{dt} \int_0^l \rho v_z(z') A_{\text{annul}}(z') dz' + \left\langle \rho v_{0z} v_0 A_{\text{sheet}} \right\rangle. \tag{7}$$

Here, F_{Nscale} is the upward normal force on the scale and the reading on the scale, $A_{\text{annul}}(z')$ is the horizontal cross-sectional area of the falling, approximately annular, water sheet at position z' below the opening, and l is the height of the falling water sheet in the CV in Fig. 4(A). (By assumption, A_{annul} is independent of time; however, A_{annul} is a function of height because the falling water accelerates.) In Eq. (7) $v_z(z') = \hat{z} \cdot \vec{v}(z')$. The total linear momentum of the collected water in the CV is nearly constant. ("Nearly" is discussed in Section 4.) However, the downward momentum of the falling water

sheet decreases with time because the bottom of the sheet is consumed by the rising water level (L) in the collection tank $dl/dt = -dL/dt$:

$$\frac{d}{dt}\int_0^l \rho v_z(z') A_{\text{annul}}(z')\,dz' = \rho v_z(l) A_{\text{annul}}(l)\frac{dl}{dt} = -\dot{m}\frac{dL}{dt} < 0 \ , \tag{8}$$

where we have used conservation of mass $\rho v_z(l) A_{\text{annul}}(l) = \langle \rho v_0 A_{\text{sheet}} \rangle = \dot{m}$. The normal force on the scale is the sum of gravitational forces and momentum change:

$$F_{\text{Nscale}} = F_{\text{grav}} + \dot{m}\left(\dot{L} + v_{0z}\right). \tag{9}$$

The scale measures the weight $F_{\text{Nscale}} = m_{\text{Cal}} g$, where m_{Cal} is the calibrated mass reading on the scale. Let m_{water} be the total mass of water in the control volume, then the gravitational force is

$$F_{\text{grav}} = m_{\text{water}}\left(1 - \rho_{\text{air}}/\rho_{\text{water}}\right) g + W_{\text{tare}} \tag{10}$$

The rate of change of the force on the scale is

$$\frac{d}{dt} F_{\text{Nscale}} = \dot{m}_{\text{water}}\left(1 - \rho_{\text{air}}/\rho_{\text{water}}\right) g + \cancel{\frac{d}{dt}\left[\dot{m}\left(\dot{L} + v_{0z}\right)\right]} \tag{11}$$

The derivative in Eq. (11) is zero because dm/dt, v_{0z} and dL/dt are all constant. dL/dt is constant because dm/dt is constant the tank cross section is independent of height. The rate of change of the mass reading from the scale is

$$\dot{m}_{\text{scale}} = \dot{m}_{\text{water}}\left(1 - \rho_{\text{air}}/\rho_{\text{water}}\right) \tag{12}$$

Equation (12) is valid for steady flows into the collection tank, even when flows persist inside the collection tank so long as the center of mass of such persistent flows has no vertical component.

As discussed by Shinder and Moldover [7], persistent flows such as internal circulation, rigid-body rotation, and symmetrical waves are consistent with Eq. (1). In contrast, a rising flow of bubbles will be accompanied by a falling center of mass that will affect the scale. Shinder and Moldover [7] extended Eq. (1) to apply to unsteady flows. However, as described in Section 4.1, the flow in the LFS primary standard is sufficiently steady that Eq. (1) applies.

As discussed in Section 6 below, the time-stamped weigh scale readings are fitted with a straight line whose slope equals the mass flow. To meet our uncertainty and stability criteria for the 15 kg/s LFS, the standard error of the slope must be less than 0.0045 %. At the minimum flow, (0.22 kg/s) the standard error in the slope is normally an order of magnitude smaller than this; however, at the maximum flow (15 kg/s) the standard error in the slope can be as large as 0.0045 % because fewer data points are collected during the shorter collection interval. If the standard error in the slope exceeds 0.0045 % during a customer calibration, the data set is rejected.

Because the flow is *steady*, the weigh scale mass versus time is a nearly straight line with the slope of the line equal to the mass flow. Herein, we use linear regression of the time-stamped weigh scale

readings to determine the slope, and hence the mass flow. The linear regression model for the slope is [15]:

$$\dot{m}_{\mathrm{LFS}} = \frac{N\sum_{i=1}^{N} m_{\mathrm{i}} t_{\mathrm{i}} - \sum_{i=1}^{N} t_{\mathrm{i}} \sum_{i=1}^{N} m_{\mathrm{i}}}{N\sum_{i=1}^{N} t_{\mathrm{i}}^2 - \left(\sum_{i=1}^{N} t_{\mathrm{i}}\right)^2}, \tag{13}$$

where t_{i} and m_{i} are the respective time and buoyancy corrected mass values from the scale, and N is the number of mass readings in the data set. We also determine the intercept:

$$c = \frac{\sum_{i=1}^{N} t_{\mathrm{i}}^2 \sum_{i=1}^{N} m_{\mathrm{i}} - \sum_{i=1}^{N} t_{\mathrm{i}} \sum_{i=1}^{N} m_{\mathrm{i}} t_{\mathrm{i}}}{N\sum_{i=1}^{N} t_{\mathrm{i}}^2 - \left(\sum_{i=1}^{N} t_{\mathrm{i}}\right)^2}, \tag{14}$$

which is used for the uncertainty analysis (Section 8).

Because some flow meters under test measure volume flow rather than mass flow, we also use an expression that relates the LFS mass flow to volume flow at the test section:

$$\dot{Q}_{\mathrm{LFS}} = \dot{m}_{\mathrm{LFS}} / \rho_{\mathrm{MUT}}, \tag{15}$$

where ρ_{MUT} is the fluid density at the MUT. The density of water is given by:

$$\rho_{\mathrm{water}} = \rho_{\mathrm{ref}} \left[1 - \beta\left(T - T_{\mathrm{ref}}\right) + \kappa\left(P - P_{\mathrm{ref}}\right)\right], \tag{16}$$

where ρ_{ref} is the density of water at T_{ref} = 294 K and P_{ref} = 101 kPa, β is the volumetric thermal expansion coefficient for water (2.1×10^{-4} 1/K), κ is the isothermal compressibility factor for water (4.6×10^{-7} 1/kPa), and T and P are the temperature and pressure of the water in the test section, respectively. The values of β and κ are taken from the literature for pure water [16]; however, they have been shown to be valid for tap water within small uncertainty [17]. For calibrating MUTs that measure volume flow, an accurate value of ρ_{ref} is required. Therefore, we take a sample of water from the collection tank and measure $\rho(T)$ using a vibrating tube densimeter. The densimeter is calibrated with air and pure water and the resulting value of ρ_{ref} has an uncertainty of 80 parts in 10^6 at the 95 % confidence level.

Others have discussed liquid flow calibration systems based on dynamic weighing [18, 19]. They noted that the water filling the collection tank delivers vertical and transverse momentum to the water already in the tank thereby driving complex flows within the tank. They consider the submerged water jet and its penetration depth, impact energy dissipated in the tank, and fluid structure interaction. These complications are circumvented by our use of a control surface and the Reynolds transport theorem in Section 5.0.

5.1 Mass flow due to storage effects in the connecting volume

During a calibration, changes in the mass of water stored in the volume between the MUT and the collection tank ($\dot{m}_{\mathrm{S}}$) are small compared with the mass flow ($\dot{m}_{\mathrm{S}} / \dot{m}_{\mathrm{LFS}} < 3 \times 10^{-6}$ at the lowest flow of

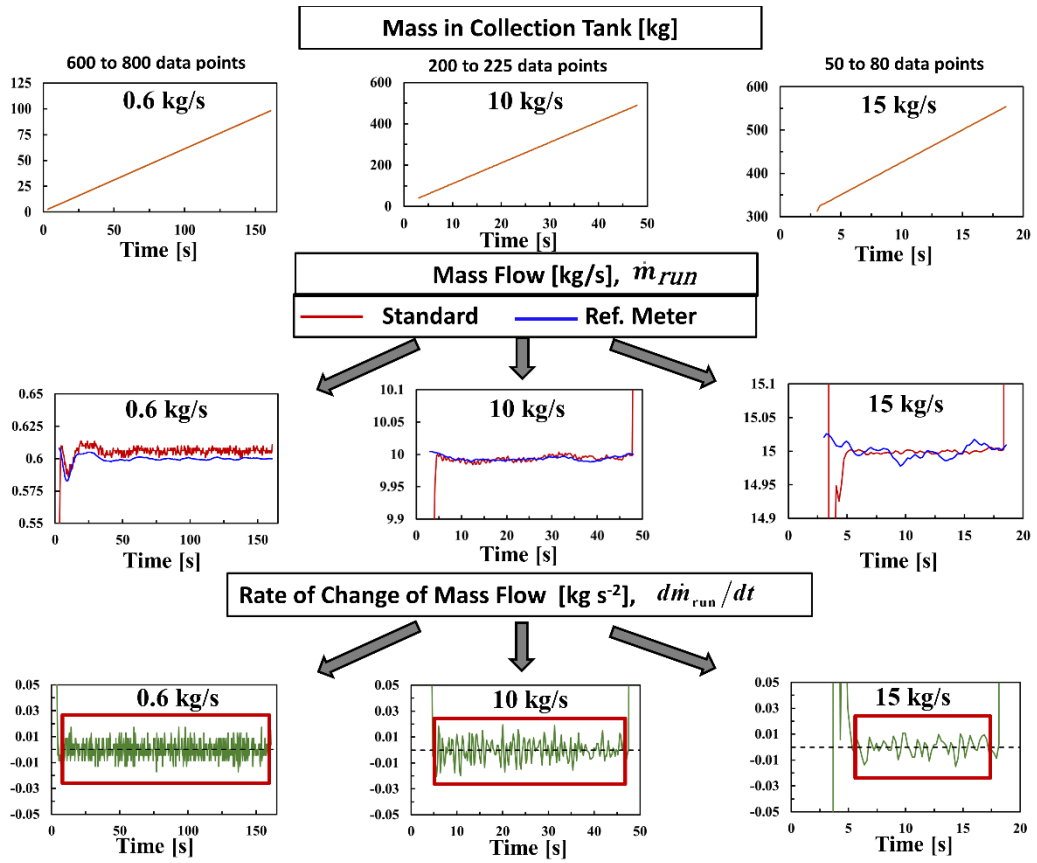

Fig. 5. Illustration of data selection. Bottom row: The red rectangles show the data that are qualified for further analysis. All curves are running averages of 30 measurements taken at intervals of 0.21 s.

0.22 kg/s). The mass of water in the connecting volume will change if either the size of the volume or the water's density changes during the interval that data are collected from the tank and the MUT:

$$\dot{m}_S = \rho \frac{dV_c}{dt} + V_c \frac{d\rho}{dt} \approx V_c \left(\rho_{final} - \rho_{initial}\right) \Big/ \sum_{i=1}^{N} t_i \qquad \text{and} \qquad t_{final} - t_{initial} = \sum_{i=1}^{N} t_i \tag{17}$$

where V_c is the size of the connecting volume. If one assumes that the connecting volume is constant, the expression simplifies to the approximation in Eq. (17) where $\rho_{initial}$ and ρ_{final} are the densities in the connecting volume at the beginning and end of the collection, and $t_{final} - t_{initial}$ is the duration of the collection period. For the LFS operating at its maximum flow of 15 kg/s, the temperature change of the water in the connecting volume during a collection is less than 0.05 K and pressure changes are less than 5 kPa which leads to $\dot{m}_S / \dot{m}_{LFS} < 3 \times 10^{-7}$.

6.0 Processing the Mass and Time Data to Calculate Flow

Figure 5 illustrates the raw data generated by the 15 kg/s LFS and its reduction to mass flow. The data shown were acquired during the calibration of a 5 cm diameter Coriolis meter. The top row of graphs plots the mass in the collection tank as a function of time as the tank filled. The first mass was recorded when the collection was started by closing the dump valve. The middle row of graphs plots a 30 point (6 s) running average of the rate of change of the mass in the collection tank $\dot{m}_{run}$, and the bottom row plots the derivative of the rate of change $d\dot{m}_{run}/dt$. The derivative was calculated numerically from the

differences between adjacent points in the running averages. We use $\dot{m}_{\text{run}}$ to represent the running-averaged mass flow and use $\dot{m}_{\text{LFS}}$ for the mass flow determined by linear regression, Eq. (13).

Strictly speaking, Eq. (13) is valid only when the flow is steady. Steady flow results in a linear mass *versus* time trace for which the slope (or mass flow) is constant. However, the flow is not perfectly steady, as evidenced by the rate of change of the mass $\dot{m}_{\text{run}}$ shown during the collection periods in Fig. 5 (middle row). Therefore, we pre-qualify the data to ensure that the slope calculation Eq. (13) uses only the portion of data where the flow is sufficiently steady to compute the slope with the desired uncertainty using linear regression. For the pre-qualification, we calculated a running average of 30 measurements of the mass and time [20]. We determined the running average mass flow $\dot{m}_{\text{run}}$ and its time derivative $d\dot{m}_{\text{run}}/dt$ throughout a collection period. These parameters are estimated using second order finite difference formulas [21] based on the scale mass readings and their corresponding time measurements. The running-averaged mass flow $\dot{m}_{\text{run}}$ and its derivative are used ***only*** to assess flow stability and to select portions of the data record that are suitable for further processing. For example, closing and opening the dump valve leads to transients in the mass *versus* time data that increase the uncertainty of $\dot{m}_{\text{LFS}}$. Examples of such mass transients can be seen in the middle row of Fig. 5. In addition, there are random motions of the water in the tank and electronic noise in the instruments that lead to fluctuations in the mass *versus* time slope. The running average dampens the random noise in the mass measurements, thereby facilitating the detection of unwanted transients.

The criteria for assessing steady flow conditions is based on the rate of change in mass flow during a collection, $d\dot{m}_{\text{run}}/dt$. The bottom row of Fig. 5 shows three plots of $d\dot{m}_{\text{run}}/dt$ during collections. Based on our experience, values of $|d\dot{m}_{\text{run}}/dt| < 0.03$ kg/s^2 indicate data that are sufficiently steady to process through Eq. (13). We also ensure that the pre-qualified mass *versus* time data are sufficiently linear by requiring that computed values of the relative standard error in the slope are less than 0.0045 %; see Eq. (24).

7.0 Comparison to NIST's Existing Liquid Flow Standards

We compared the 15 kg/s LFS to two of NIST's previously documented liquid flow standards: the 65 kg/s dynamic gravimetric standard [22] and the 2.5 L/s piston prover [23]. Figure 6 shows the results of the comparisons using 5 cm and 2.5 cm Coriolis mass flow meters as transfer standards. The larger transfer standard was calibrated on the 15 kg/s LFS and the 65 kg/s standards. The smaller transfer standard was calibrated on the 15 kg/s LFS and the 2.5 L/s LFS. The vertical uncertainty bars represent the expanded uncertainty, approximately 95 % confidence level, of each standard (0.022 % for the 15 kg/s LFS, 0.033 % for the 65 kg/s LFS, and 0.064 % for the 2.5 L/s LFS) summed in quadrature with twice the standard deviation of the mean of at least three repeated comparisons. The 15 kg/s LFS agrees with the existing standards well within their uncertainties.

Figure 7 shows the standardized degree of equivalence E_{n} for these internal comparisons. They are consistent with the claimed capabilities of all three primary standards, as demonstrated by values of $E_{\text{n}} < 1$. The standardized degree of equivalence is:

$$E_{\text{n}} = \frac{\left(\dfrac{\dot{m}_{\text{15 kg/s LFS}}}{\dot{m}_{\text{MUT, 15 kg/s}}} \Big/ \dfrac{\dot{m}_{\text{STD}}}{\dot{m}_{\text{MUT, STD}}} - 1 \right)}{\sqrt{U^2_{\text{15 kg/s LFS}} + U^2_{\text{STD}} + U^2_{\text{MUT}}}} \tag{18}$$

In Eq. (18), $\dot{m}$ is the mass flow; the subscript STD denotes either the 65 kg/s or the 2.5 L/s LFS; the subscript MUT denotes one of the transfer standards and $U_{\mathrm{MUT}} = 2s/\sqrt{N}$ is the fractional expanded

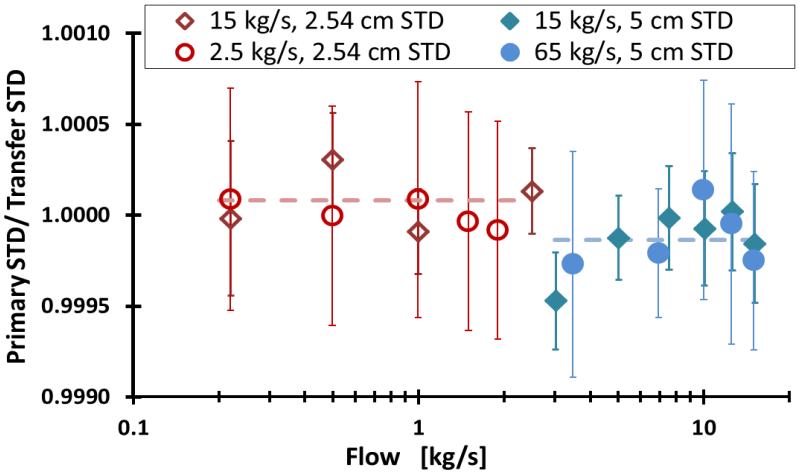

Fig 6. Ratios of flows determined by the new 15 kg/s LFS to flows determined by NIST's 65 kg/s and 2.5 L/s liquid flow standards using 5 cm transfer standard (solid symbols) and 2.5 cm transfer standard (open symbols). The pink and the blue dashed lines are the unweighted mean results from the 2.5 cm and the 5 cm transfer standards, respectively. Each vertical bar is the expanded uncertainty of a comparison.

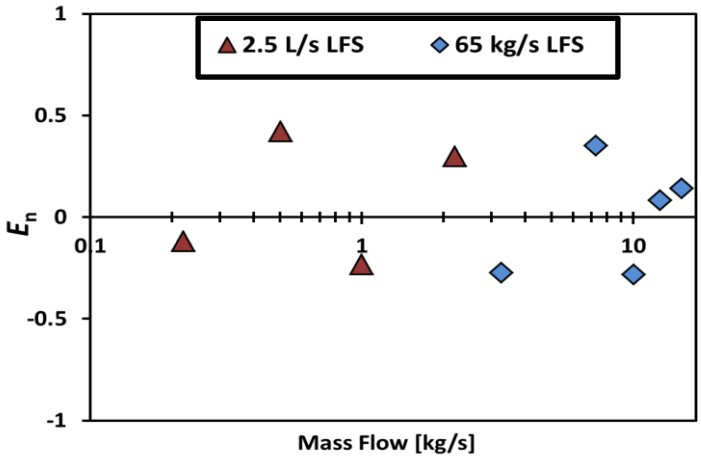

Fig. 7. Degrees of equivalence for two meters used in a comparison between the 15 kg/s LFS and the 65 kg/s LFS (blue diamonds) and the 2.5 L/s LFS (red triangles). A 5 cm Coriolis meter was used for comparison with the 65 kg/s LFS; a 2.5 cm Coriolis meter was used for the 2.5 L/s LFS comparison.

uncertainty of the transfer standard. The reproducibilities of both the 5 cm and the 2.5 cm transfer standards were $s/\sqrt{N}$ = 0.021 %, where s was the standard deviation of the mean of N repeated measurements made on the 15 kg/s LFS before and after the comparison.

8.0 Uncertainty

This uncertainty analysis will assess: 1) $u(\dot{m}_{\mathrm{LFS}})$ the uncertainty of the mass flow in the test section of the LFS, 2) $u(Q_{\mathrm{LFS}})$ the uncertainty of the volumetric flow in the test section of the LFS, and 3) $\dot{m}_{\mathrm{S}}$ the mass flow from the connecting volume. The uncertainty components associated with these quantities

are discussed in detail in the following sections. As seen in Eqns.(13), (15), and (17) they include the uncertainty contributions from the following elements:

a) The uncertainty of the slope determining $\dot{m}_{LFS}$ by regressing the time-stamped mass readings;
b) The mass (m_i) and time (t_i) measurements used for the linear regression analysis given in Eq. (13);
c) Buoyancy corrections to the mass readings, ρ_{air}, and ρ_{water};
d) Mass storage in the connecting volume, $\rho_{initial}$, ρ_{final}, and V_c;
e) The water density at the MUT, ρ_{MUT}.

Table 2. Uncertainty budget for the mass flow and volume flow in the test section of the LFS. The data listed are for a nominal flow of 15 kg/s; however, the uncertainty is independent of flow. The yellow highlighted cells correspond to the yellow highlighted cells in Table 3.

Contribution to $U^a(\dot{m}_{LFS})$	Nominal Value	S_{xi}[b] [-]	$u(x_i)$[c] [%]	$S_{xi}^2 u(x_i)^2$	Unc. Type	Contribution to $U(\dot{m}_{LFS})$ [%]	$u_c(\dot{m}_{LFS})$[d] [%]
m_i [kg] (calibration)	–	1	0.01	1.0×10^{-4}	B	82.84	**0.011**
m_i [kg] (resolution)	–	1	4.1×10^{-4}	1.7×10^{-9}	B	<0.01	
m_i [kg] (zero drift)	–	1	4.1×10^{-5}	1.7×10^{-11}	B	<0.01	
ρ_{air} [kg/m^3]	1.17	0.0012	0.39	2.1×10^{-7}	B	0.18	
ρ_{H2O} [kg/m^3]	995.92	-0.001	0.004	2.2×10^{-11}	B	< 0.01	
Slope (Regression) [kg/s]	15	1	0.0045	2.0×10^{-5}	A	16.78	
$\dot{m}_S$ [kg/s]	4.1×10^{-6}	2.7×10^{-7}	26.30	5.1×10^{-11}	B	< 0.01	
τ[e] [s]	0.209718	1	5.0×10^{-4}	2.5×10^{-7}	A&B	0.21	
Contribution to $U(\dot{Q}_{LFS})$	**Nominal Value**	**S_{xi} [-]**	**$u(x_i)$ [%]**	**$S_{xi}^2 u(x_i)^2$**	**Unc. Type**	**Contribution to $U(\dot{Q}_{LFS})$ [%]**	**$u_c(\dot{Q}_{LFS})$ [%]**
$\dot{m}_{LFS}$ [kg/s]	15	1	0.011	1.2×10^{-4}	B	88.30	**0.012**
ρ_{MUT} [kg/m^3]	995.92	1	0.004	1.6×10^{-5}	B	11.70	

[a] U is the combined, approximately 95 % confidence level relative uncertainty ($k = 2$). Section 8.1.
[b] S_{xi} is the normalized sensitivity coefficient, Section 8.1. Formulas are given in Appendix B.
[c] $u(x_i)$ is the relative, standard uncertainty of variable x_i listed in the leftmost column, Section 8.1
[d] u_c is the combined, approximately 68 % confidence level, relative uncertainty ($k = 1$), Section 8.1.
[e] τ is the interval between weigh scale readings. $N\tau$ is therefore, the collection time.

As shown in Table 2, the largest contributors to the uncertainty of the mass flow $u(\dot{m}_{LFS})$ are the weigh scale calibration and the regression of the weigh scale readings to a linear function. All other contributors to $u(\dot{m}_{LFS})$ total to only 0.30 % of $u(\dot{m}_{LFS})$ and therefore are ignored in this overview. Our analysis shows that the expanded uncertainties of the mass flow and volumetric flow at the MUT are

0.022% and 0.030 %, respectively. The operating requirements of the LFS (minimum collected mass of 44 kg, minimum collection time of 15 s, pre-qualification of data for flow stability, *etc*.) ensure that the LFS uncertainty is independent of the flow over the entire operating range.

First, we outline the uncertainty methods and formulas that will be used (Section 8.1). Next, we assess all the sub-measurement uncertainty components necessary to calculate the uncertainty in the mass and volume flows (Sections 8.2 and 8.3). The expanded uncertainty of the MUT calibration factor is documented in Section 8.4, and the additional uncertainty considerations for a customer's MUT are discussed in Section 8.5.

8.1 Techniques for uncertainty analysis

Here we follow the guidelines for evaluating and expressing uncertainty provided in NIST TN 1297 [24], the ISO Guide to Uncertainty in Measurement [4], and elsewhere [15]. In general, a data reduction equation is used to relate the measurand, y , (which is not directly measured) to n measured input variables,[iv] x_i :

$$y = f\left(x_1, x_2, \ldots..., x_n\right), \tag{19}$$

where each x_i has a relative standard uncertainty of $u(x_i)$.[v] The combined relative standard uncertainty of the measurand, $u\,(y)$, can either be calculated numerically via a Monte Carlo simulation [15], or analytically via the propagation of uncertainty formula:

$$u^2(y) = \sum_{i=1}^{n} S_{x_i}^2 u^2(x_i) + 2\sum_{i=1}^{n-1}\sum_{j=i+1}^{n} S_{x_i} S_{x_j} r_{ij} u(x_i) u(x_j) \tag{20}$$

where $S_{x_i} = \left(\partial y / \partial x_i\right) x_i / y$ is the dimensionless sensitivity coefficient of x_i on y , and $r_{i,j}$ is the correlation coefficient between variables x_i and x_j, which, depending on the degree of correlation, has a value between -1 and 1. Equation (20) is based on a truncated, linear Taylor series of the data reduction equation. For the special case of uncorrelated uncertainties ($r_{i,j}$ =0), Eq. (20) simplifies to the root-sum-square (RSS) of the uncorrelated components:

$$u^2(y) = \sum_{i=1}^{n} S_{x_i}^2 u^2(x_i) \tag{21}$$

Note that the equations for flow from the dynamic gravimetric standard (Eqns. (13) and (15)) have differences between terms. These terms offer opportunities for uncertainty reduction if the mass and time measurements are positively correlated. For example, a constant zero offset in the weigh scale reading would cancel out when the subtraction $m_2 - m_1$ is carried out. However, the significant uncertainty components for mass and time are errors in slope and calibration factors that are not correlated (not zero offsets). The zero-offset uncertainty in the weigh scale is also uncorrelated because we are including only the change in the zero that might occur during the course of a collection. We therefore used Eq. (21).

[iv] The variable n in Eqns. (19) through (21) is the number of variables in the data reduction equation. It should not be confused with N in Eqns. (13),(14), and (17) which is the number of scale readings in a collection.

[v] The relative standard uncertainty (sometimes referred to as the standard normalized uncertainty) is the absolute uncertainty at the 68 % confidence level divided by x_i.

We used an independent Monte Carlo analysis (not described herein) to confirm that the uncertainty calculations made using Eq. (21) were accurate. In accordance with [4] we categorized the uncertainty components into *Type A* – those that are evaluated by statistical methods, and *Type B* – those that are evaluated by other means. In cases where x_i could not be directly measured, but was calculated via its own data reduction equation, we used the propagation of uncertainty formula to compute $u(x_i)$.

8.2 Contributions to the relative standard uncertainties of the mass and volume flow

The relative standard uncertainties contributing to mass and volume flow are itemized in Tables 2 and 3. The tables show that the largest uncertainty sources in $\dot{m}_{\mathrm{LFS}}$ include the weigh scale mass calibration (82.82 %), and the regression error in the slope calculation (16.77 %), which together contribute > 99 % of the mass flow uncertainty and > 88.30 % of the volume flow uncertainty. Although the remaining uncertainty components (*i.e.*, scale resolution, buoyancy corrections, and mass storage effects) make negligible contributions to the overall mass flow uncertainty, we document these smaller uncertainty components along with the larger components in Sections 8.2.a through 8.2.c for completeness. In Section 8.2.d we document the liquid density uncertainty because it makes a significant contribution to the overall uncertainty in the volume flow at the MUT, $\dot{Q}_{\mathrm{LFS}}$.

8.2.a. Mass and time measurements

Weigh Scale Calibration, Resolution, and Zero Drift

The weigh scale is tared when the collection tank is empty and resting on it; therefore, all scale readings, or loads, are relative to the tare value. The weigh scale was calibrated over the range of 90 kg to 650 kg when the laboratory temperature was approximately 19 °C and 23 °C. During these calibrations, the effects of temperature on the scale calibration were negligible (*i.e.* < 1 part in 10^6). At the time of this publication, the weigh scale has been calibrated four times. Considering the uncertainty from the reference masses and the repeatability of the calibrations, the weigh scale's calibration has an expanded uncertainty of 0.02 %.

The calibration of the weigh scale used a sequential, incremental-loading method based on two NIST-calibrated 45 kg masses. We calibrated the 45 kg masses using reference masses (*i.e.*, a 65 kg weight set that is traceable to the SI) and a 60 kg-capacity mass comparator from NIST's Liquid Volume Calibration Service [17]. The 45 kg masses were calibrated in the same room where they were used to calibrate the weigh scale. Therefore, the location-dependence (and smaller time-dependence) of g made negligible contributions to the calibration uncertainty.

A bootstrap method was implemented to span the entire 600 kg range of the scale using only the two 45 kg masses. After taking calibration data with both 45 kg masses on the scale, we replaced the two 45 kg masses with approximately 90 kg of water in the collection tank and recorded the scale reading. With the water remaining in the collection tank, we again placed the two 45 kg masses onto the scale. The difference of the last two scale readings was the change due to the force applied by the 45 kg masses. In this way, we sequentially progressed through the weigh scale's range in 90 kg increments calculating a calibration factor as a function of scale reading. The weigh scale calibration factor is defined as the force applied by the reference masses divided by the force indicated by the weigh scale: $m_a g/W$ where m_a is the buoyancy corrected (or apparent) mass of the 45 kg reference masses. The expanded uncertainty of the measurement is 0.02 %, which includes the *Type-B* uncertainty in the calibration of the two reference masses (0.0011 %, $k = 2$) and the standard deviation of the four repeated calibrations (0.003 % to 0.007 %, $k = 2$). This is the largest source of uncertainty for flow measurements made with the LFS. Equation (22) shows how the calibration factor is applied to the weigh scale readings:

$$m_{\text{cal}} = \text{Cal Factor} \times \left(\frac{W}{g(1-\rho_{\text{air}}/\rho_{\text{H}_2\text{O}})} \right), \tag{22}$$

where Cal Factor = 0.99965 ± 2.0×10^{-4} and m_{cal} is the calibrated, buoyancy corrected mass on the weigh scale. Figure 8 shows the deviations of the weigh scale calibration factors from the average versus the scale reading. The values of W/g are the average of the weigh scale readings for each 90 kg increment.

As previously explained, correlation between the multiple mass measurements made in a flow measurement would be an important consideration if there was a significant and stable zero offset in the weigh scale: the zero error would "cancel out" during the subtraction process. But in this case, the scale is tared, and the important mass uncertainty sources (zero drift during a single flow measurement and the scale calibration factor) are not well correlated. Therefore, we conservatively assume that there is no correlation between the time-stamped mass measurements.

The resolution of the weigh scale output is 10 g. The weigh scale resolution for sequential mass measurements is an uncorrelated *Type-B* source of uncertainty because the resolution introduces noise in the scale that causes scale readings to be high or low by 5 g. The resolution errors are treated conservatively as having a rectangular distribution and as an uncorrelated uncertainty and contribute < 0.01 % (Table 2) to the mass flow uncertainty budget. To achieve this acceptable level of uncertainty due to scale resolution, it is necessary to collect a minimum of only 44 kg of water for a single flow measurement.

The weigh scale's zero stability (W_{tare}) was assessed by recording the scale's readings with two different loads, 1) the empty collection tank, and 2) the empty collection tank plus two 45 kg masses. The durations of these two tests were 2000 min and 1500 min, respectively. The laboratory's temperature was also recorded to detect a possible temperature-dependence of W_{tare}. The laboratory temperature ranged from 16 °C to 20.2 °C between the tests and had a negligible effect on W_{tare}. The maximum zero drift observed in the drift tests was 0.3 g/min. Based on this result, we estimate the standard uncertainty introduced by zero drift in the balance over the 200 s maximum collection time is 1 g. The zero drift component is a negligible contributor to the mass flow uncertainty (< 0.01 %, see Table 2).

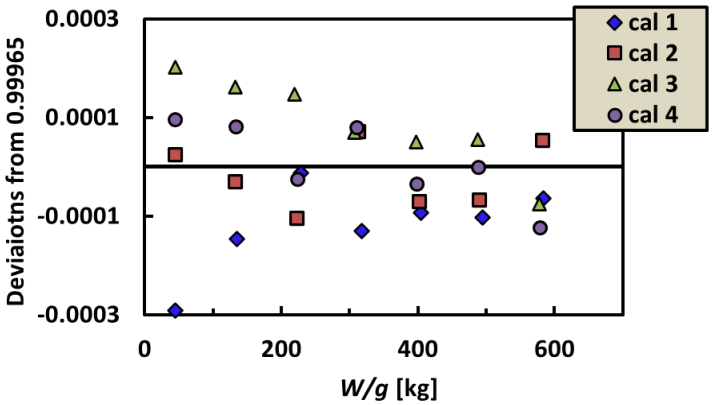

Fig. 8. Deviations between individually measured weigh scale calibration factors and the average of all measurements, 0.99965. The values of W/g are the average of the weigh scale readings for each 90 kg increment.

Dynamic Response and Load Dependence of the Weigh Scale

Our procedure for calibrating the weigh scale is valid for static weightings. However, during customer calibrations, the 15 kg/s LFS measures a constantly-increasing collected mass. Therefore, we searched for measurement errors that might arise from dynamic weighing. According to the weigh scale's manufacturer, the update rate of the weigh scale is 6 Hz; therefore, we did not expect to see effects due to an excessively long scale response time. A plausible model for the weigh scale's response is that of an underdamped harmonic oscillator subjected to a changing load. If the scale oscillates, the envelope of the oscillations will decay towards its final value with a time constant time $\tau_{\text{damping}} \propto$ (mass)/(damping constant). As mass accumulates on the scale, τ_{damping} increases and the lag between indicated load and the true load increases, thereby generating an underestimate (bias) of $\dot{m}_{\text{LFS}}$ that increases with the mass of water collected.

To search for mass-dependent bias, we compared the mass of water delivered according to the reference Coriolis meter to the mass measured by the weigh scale during a 30 second, 60 second, and 120 second collection periods. During the collections, we assumed that the flow rate and the Coriolis meter's calibration factor were constant. (The water's temperature increased by less than 0.05 K.) We compared the integrated output of the Coriolis meter to the buoyancy-corrected weigh scale readings, Eqn. (23). In effect, this was a calibration of the Coriolis meter.

$$\Delta m = (m_{\text{cal},i+1} - m_{\text{cal},i}) - \int_{t_i}^{t_{i+1}} \dot{m}_{\text{meter}}\, dt \cong 0 \tag{23}$$

Figure 9A shows the relationship between m_{cal} and the mass metered by the reference meter as the scale is loaded from approximately 220 kg to over 570 kg at a rate of approximately 15 kg/s. The solid line is the measured data; the dashed line is what the relationship would look like for a postulated load dependent delay in the response time that increases as the load on the weigh scale increases. The load dependent weigh scale response is modeled using a second-order polynomial fit to the weigh scale reading *versus* time data and increasing the second-order term by a factor of 100. Figure 9B shows Δm for the measured data and the postulated data in Fig. 9A. If a load dependent response dampened the weigh scale output, deviations like those seen in Fig. 9B for the postulated data would occur in real data; however, we have exaggerated the effect in our example.

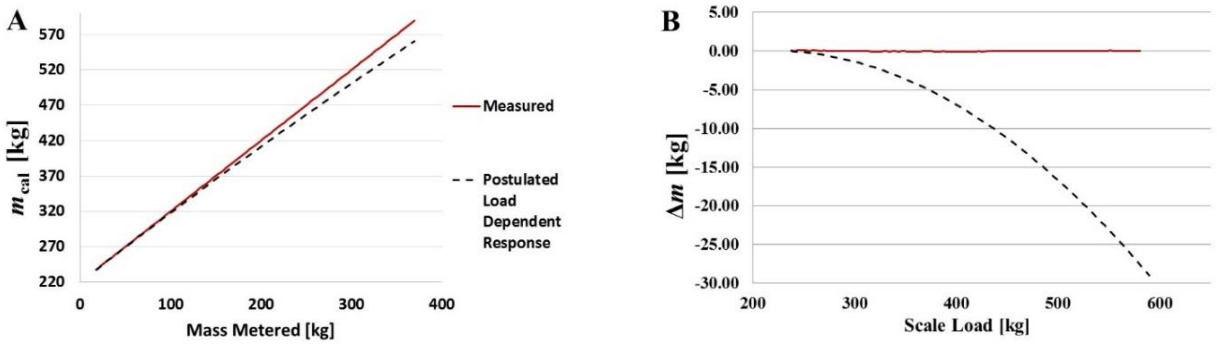

Fig. 9. A) Relationship between m_{cal} and the mass metered by the reference meter as the scale is loaded from approximately 220 kg to over 570 kg. B) Difference in m_{cal} and the mass metered by the reference meter for both cases in (A). The solid lines are the real, measured data; the dashed lines are the postulated data assuming a load dependent delay in the weigh scale response time.

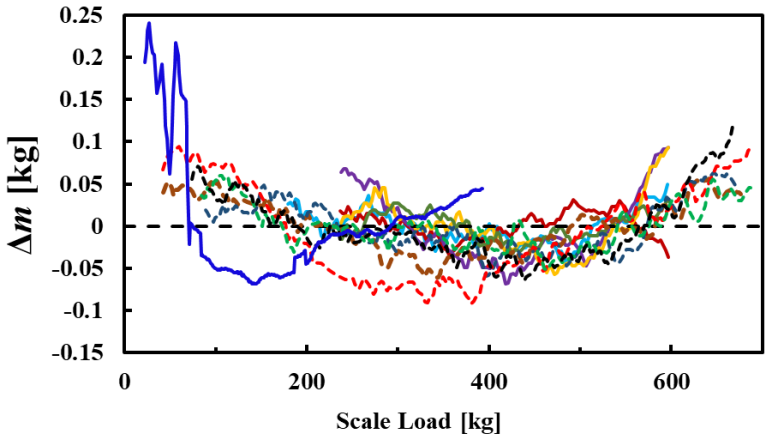

Fig. 10. The difference in mass measured by the weigh scale m_{cal} and the reference Coriolis meter as the collection tank fills at 13.5 kg/s, 10.5 kg/s, and 3 kg/s.

Figure 10 shows multiple sets of data consisting of five repeated calibration points at 13.5 kg/s and 10.5 kg/s and one calibration point at 3 kg/s. Equation (23) was used to compare m_{cal} to that measured by the reference meter. The Δm values are distributed around zero with a noticeable curvature, however, not seemingly load dependent. For a calibration, it is the sum of the mass increments that determine the meter's calibration. If the differences in Fig. 10 are summed and divided by the total collected mass: $\sum_{i=1}^{N}\left[(m_{\text{cal},i+1}-m_{\text{cal},i})-\int_{t_i}^{t_{i+1}}\dot{m}_{\text{meter}}dt\right]\Big/m_N$, the largest ratio observed is 6×10^{-14}. Therefore, given the results of our tests, we conclude that the effects of weigh scale load on the response time of the scale is not detectable in our system.

Uncertainty of the slope determination

Provided the flow is steady, the slope (and therefore the mass flow) can be accurately calculated by the linear regression formula given in Eq. (13). After pre-qualifying the data as explained in Section 6.0, the uncertainty in the slope (or standard error of the slope) is calculated by:

$$u(\text{slope}) = \left(\frac{u^2(\text{reg})}{S_{xx}}\right)^{1/2}, \tag{24}$$

where u(reg) is the standard error of regression:

$$u(\text{reg}) = \left(\frac{\sum_{i=1}^{N}\left(m_i - \dot{m}_{\text{LFS}}t_i - c\right)^2}{N-2}\right)^{1/2}, \tag{25}$$

where c is the intercept given in Eq. (14) and S_{xx} is a normalizing factor [15] equal to:

$$S_{xx} = \sum_{i=1}^{N} t_i^2 - \frac{1}{N}\left(\sum_{i=1}^{N} t_i\right)^2. \tag{26}$$

For an acceptable calibration using the 15 kg/s LFS, we require that the calculated uncertainty u(slope) < 0.000045×slope for each collection. If u(slope) is above this threshold we repeat the collection.

Timing uncertainty

The standard error of the slope in Eq. (13) assumes that the uncertainty of the time measurements is negligible compared to the uncertainty of the mass values. This is true: The relative standard uncertainty of the time interval measurement is 5.0×10^{-4} % of the interval, which contributes 0.21 % to the overall LFS mass flow uncertainty (Table 2).

We assessed the stability of the weigh scale clock and the data acquisition clock on multiple occasions over a three-year period with the scale loaded (610 kg above the tare weight) and unloaded (only the tare weight on the weigh scale). This assessment is repeated prior to a customer calibration. The period of the weigh scale internal 24 MHZ clock was measured by counting mass readings via LabVIEW[iii] over a total time of 1 h or more. The total time was measured using 1) a high precision (HP) counter and frequency generator, both with standard *Type-B* uncertainties of 1×10^{-4} % of the reading, 2) a National Instruments data acquisition board clock (cDAQ) with standard *Type-B* uncertainty of 0.0025 % of the reading, and 3) the Microsoft application-programming interface: Query Precision Counter (QPC) with standard *Type-B* uncertainty of 2.4×10^{-4} % of the reading. The period of the 24 MHz clock (τ) was calculated by dividing the total time by the integer number of scale output readings minus one.

Figure 11A shows τ determined by each of the clocks/counters mentioned above with the error bars showing the expanded uncertainty in each measurement. Ultimately, we used τ determined by the high precision counter because it has the lowest uncertainty of the three counters. Figure 11B shows τ determined using the HP counter between 2013 and 2016: τ = 209.7182 ms with standard deviation of 0.23 µs. The control limits are conservatively set to 209.7181 ms ± 1 µs. As long as the measured times remain inside these conservative control limits the contribution to the overall uncertainty is < 0.21 %. The standard deviation of the repeated measurements is root-sum-squared with the *Type-B* uncertainty from the HP counter, so that the relative standard uncertainty is 5.0×10^{-4} % of τ. During a calibration we take τ between scale readings as a constant and determine the time at the i^{th} scale reading using the expression $t_i = i\,\tau$. The time interval τ is a fixed value and the change in mass flow with respect to τ is unity, hence a 1 % uncertainty in τ leads to a 1 % uncertainty in mass flow.

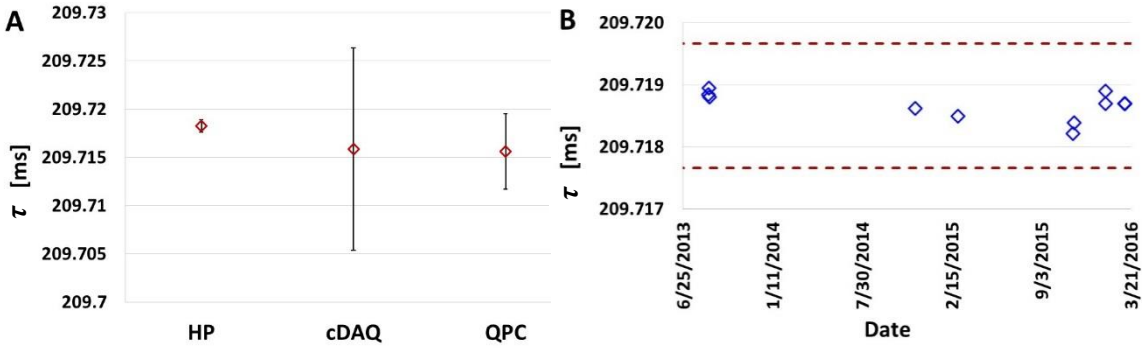

Fig. 11. A) Time increment between weigh scale readings determined by three counters/clocks. B) Control chart for the time increment per weigh scale reading as determined by the HP counter in (A). The red lines are the upper and lower control limits, 1 µs.

8.2.b. Buoyancy corrections

As shown in Eq. (1), the buoyancy correction to the mass flow $\dot{m}_{\mathrm{LFS}}$ is made by dividing the weigh scale readings by the term $(1 - \rho_{\mathrm{air}}/\rho_{\mathrm{water}})$, where $\rho_{\mathrm{air}}/\rho_{\mathrm{water}}. \approx 0.0012$ in NIST's flow laboratory. Therefore, the relative uncertainty of $u(\rho_{\mathrm{air}}/\rho_{\mathrm{water}})$ must be less than .08 to obtain a mass flow uncertainty $u(\dot{m}_{\mathrm{LFS}}) \leq 10^{-4}$. The correlation [25]

$$\frac{\rho_{\mathrm{air}}}{\mathrm{kg\ m^{-3}}} = \frac{3.4848 \times 10^{-3}}{T / \mathrm{K}} \left[\frac{P}{\mathrm{Pa}} - 6.65287 \times 10^{8}\, RH \times \exp\left(\frac{-5315.56\ \mathrm{K}}{T} \right) \right] \tag{27}$$

computes the density of air with the standard uncertainty 0.001 ρ_{air}. However, *P*, *RH* (the relative humidity expressed in percent), and *T* are measured by environmental monitors in NIST's flow laboratory. The standard uncertainty (68 % confidence level) of these environmental monitors is 0.003 *P*, 0.1 *RH*, and 0.002 *T*, as determined using NIST reference standards and control charts generated during years of calibrations. Because these uncertainty components are uncorrelated with each other, we used Eq. (21) to calculate the uncertainty of ρ_{air}. The result is a *Type B* standard uncertainty $0.0039\rho_{\mathrm{air}}$ (Table 3).

Equation (16) is used to calculate the density of the water in the collection tank. For each volume calibration, we determine ρ_{ref} in Eq. (16) by using a vibrating tube densimeter to measure the density of a water sample drawn from the collection tank. The densimeter is calibrated with air-saturated pure water and the resulting densities have a standard uncertainty of 80 parts in 10^6 at the 95 % confidence level. Typically, the measured densities are 0.02 % larger than those of pure water, probably because the tap water that is used in the flow standard contains dissolved solids.

The thermal expansion coefficient for pure water, β = 0.00021 / °C, has a standard uncertainty of 0.0015 % for pure water [26], and these values also apply to tap water. (The impurities found in tap water produce an
offset in density from pure water but have negligible effect on thermal expansion.) The REFPROP [16] database is used to compute the isothermal compressibility κ for pure water and we assumed a conservative standard uncertainty of 10 % in κ because of the use of tap water. The pressure corrections are small since the water in the collection tank is open to the atmospheric pressure in the calibration facility. As such, the corresponding uncertainties are negligible. The standard uncertainty of the tank water temperature measurement is 0.10 % of the kelvin temperature. This uncertainty comprises a 10 mK sensor calibration uncertainty added in quadrature with a 1 K sampling error uncertainty. The 1 K sampling uncertainty accounts for spatial variance we measured in the collection tank of the 15 kg/s LFS. The 1 K temperature difference is the maximum expected variation for a collection, and accordingly we use a rectangular distribution. Applying the propagation of uncertainty given in Eq. (21) for uncorrelated uncertainty components to the data reduction equation for ρ_{water} results in a combined relative standard uncertainty of 0.004 % (Table 3).

8.2.c. Mass storage in the connecting volume

The effective flow rate due to a change of mass stored in the connecting volume between the MUT and the collection tank can be computed by substituting Eq. (16) into Eq. (17):

$$\dot{m}_{\mathrm{S}} = V_{\mathrm{S}}\, \rho_{\mathrm{ref}} \left[\, \kappa\, \Delta P_{\mathrm{fi}} - \beta\, \Delta T_{\mathrm{fi}} \,\right] \Big/ \sum_{i=1}^{N} t_i \tag{28}$$

The density change is expressed in terms of the change in in the connecting volume ($\Delta T_{\mathrm{fi}} = T_{\mathrm{f}} - T_{\mathrm{i}}$), the change in the spatially averaged pressure in the connecting volume ($\Delta P_{\mathrm{fi}} = P_{\mathrm{f}} - P_{\mathrm{i}}$), the reference density ρ_{ref} , and the thermodynamic parameters β and .

The PID controller described in Sections 1.0 and 4.1 maintains the pressure to within 5 kPa at the MUT and in the connecting volume. Assuming a rectangular distribution leads to a standard uncertainty of 5 kPa / $(2\sqrt{3})$ which is equivalent to 29 % of 5 kPa[vi]. The good pressure control in our system, combined with the low compressibility of liquid water, cause the uncertainty due to the density of the water in the connecting volume to contribute less than 4.0 % to the total uncertainty due to the storage volume (Table 3).

The uncertainty attributed to changes in the average temperature in the connecting volume between the start and finish of a collection was determined experimentally. We measured the average temperature using the arithmetic average of the two temperature sensors in the connecting volume (see Fig. 1). A 0.05 K maximum temperature change was observed during a collection. We assumed a rectangular distribution in the same manner as the pressure change so that the standard uncertainty of the temperature is 0.05 K / $(2\sqrt{3})$ which is equivalent to 29 % of 0.05 K[vi].

The size of the connecting volume was determined by measuring the length and diameter of the piping between the MUT and the pipe exit leading to the collection tank (Fig. 1). This volume is approximately 0.0095 m^3 with a standard uncertainty of 10 %.

The duration of the collection is determined by multiplying the number of scale readings (N) by the time interval (τ = 209.7181 ms), that is: $\sum_{i=1}^{N} t_i = N\tau$. Section 8.2.a gives the relative standard uncertainty of the time interval between time readings as 5.0×10^{-4} %. Because collection time is proportional to τ, its relative standard uncertainty is also 5.0×10^{-4} %.

The uncertainty of the reference density of water (ρ_{ref}), the thermal expansion coefficient (β), and the isothermal compressibility (κ) are described in Section 8.2.b.

Applying the propagation of uncertainty in Eq. (21) to $\dot{m}_{\mathrm{S}}$ gives the relative uncertainty as:[vii]

$$u^2\left(\dot{m}_{\mathrm{S}}\right) = S_{\rho_{\mathrm{ref}}}^2 u^2\left(\rho_{\mathrm{ref}}\right) + S_{\Delta T_{\mathrm{if}}}^2 u^2\left(\Delta T_{\mathrm{fi}}\right) + S_{\Delta P_{\mathrm{if}}}^2 u^2\left(\Delta P_{\mathrm{fi}}\right) + S_{\beta}^2 u^2\left(\beta\right) + S_{\kappa}^2 u^2\left(\kappa\right) + S_{V_{\mathrm{S}}}^2 u^2\left(V_{\mathrm{S}}\right) + S_{\tau}^2 u^2\left(\tau\right). \tag{29}$$

Therefore, the relative standard uncertainty due to mass storage in the connecting volume is 26 %, but this contributes less than 0.01 % to the uncertainty of the mass flow $\dot{m}_{\mathrm{LFS}}$, as shown in Table 2.

[vi] [RFB: Your original wording made me think that T was correlated with P.] For the difference between the start and end of a collection, both the pressure and the temperature uncertainties are almost perfectly correlated and thus cancel. The correlation results because 1) the same two sensors are used to measure the average pressure and temperature conditions at the start and end of a collection, and 2) the initial and final conditions are nominally the same.

[vii] Appendix B gives the analytic equations for the normalized sensitivity coefficients.

Table 3. Sub-measurements and their uncertainties. The data shown are for a nominal flow of 15 kg/s, however, the uncertainty is not a strong function of flow. The yellow highlighted cells correspond to the yellow highlighted cells in Table 2. The uncertainty in the local acceleration due to gravity is negligible (< 1 part in 10^6).

Contribution to $U(\rho_{water})$	Nominal Value	S_{xi} [-]	$u(x_i)$ [%]	$S_{xi}^2 u(x_i)^2$	Unc. Type	Contribution to $U(\rho_{water})$ [%]	$u_c(\rho_{water})$ [%]
ρ_{ref} [kg/m^3]	997.995	1	0.004	1.6×10^{-5}	B	>99.99	**0.004**
β [1/°C]	2.1×10^{-4}	-6.1×10^{-3}	0.015	9.2×10^{-9}	B	<0.01	
T [°C]	29.08	-6.1×10^{-3}	0.10	3.4×10^{-7}	B	<0.01	
Contribution to $U(\rho_{air})$	**Nominal Value**	**S_{xi} [-]**	**$u(x_i)$ [%]**	**$S_{xi}^2 u(x_i)^2$**	**Unc. Type**	**Contribution to $U(\rho_{air})$ [%]**	**$u_c(\rho_{air})$ [%]**
T [°C]	21	-1.11	0.20	0.048	B	30.67	**0.39**
P [kPa]	101.325	1.03	0.3	0.095	B	61.57	
RH [%]	50	-0.005	10	0.002	B	1.31	
Equation of State	-	1	0.1	0.01	B	6.46	
Contribution to $U(\rho_{MUT})$	**Nominal Value**	**S_{xi} [-]**	**$u(x_i)$ [%]**	**$S_{xi}^2 u(x_i)^2$**	**Unc. Type**	**Contribution to $U(\rho_{MUT})$ [%]**	**$u_c(\rho_{MUT})$ [%]**
ρ_{ref} [kg/m^3]	997.995	1	0.004	1.6×10^{-5}	B	99.74	**0.004**
T [°C]	23	-1.7×10^{-3}	0.019	1.1×10^{-9}	B	<0.01	
P [kPa]	234.84	6.1×10^{-5}	0.05	9.3×10^{-12}	B	< 0.01	
β [1/°C]	2.1×10^{-4}	-1.7×10^{-3}	0.015	7.1×10^{-10}	B	< 0.01	
κ [1/kPa]	4.6×10^{-7}	6.1×10^{-5}	10	3.7×10^{-7}	B	2.28	
Contribution to $U(\dot{m}_S)$	**Nominal Value**	**S_{xi} [-]**	**$u(x_i)$ [%]**	**$S_{xi}^2 u(x_i)^2$**	**Unc. Type**	**Contribution to $U(\dot{m}_S)$ [%]**	**$u_c(\dot{m}_S)$ [%]**
ρ_{ref} [kg/m^3]	997.995	1	0.004	1.6×10^{-5}	B	< 0.01	**26.30**
ΔT_{fi} [°C]	0.05	0.82	28.87	5.6×10^{2}	B	81.24	
ΔP_{fi} [kPa]	5	0.18	28.87	26	B	3.85	
β [1/°C]	2.1×10^{-4}	0.82	0.016	1.7×10^{-4}	B	<0.01	
κ [1/kPa]	4.6×10^{-7}	0.18	10	3.19	B	0.46	
V_S [m^3]	0.0095	1	10	100	B	14.45	
τ [s]	0.209718	1	0.0005	2.5×10^{-7}	B	< 0.01	

8.2.d. Water density at the MUT

Calibrations of volume flow meters such as turbine and positive displacement meters require us to determine the water density at the LFS test section. Equation (16) is used to calculate the water density from temperature and pressure measurements. Following Eq. (21) the combined relative uncertainty is the RSS of the sub-measurement components:[vii]

$$u^2\left(\rho_{\mathrm{MUT}}\right)=S_{\rho_{\mathrm{ref}}}^2u^2\left(\rho_{\mathrm{ref}}\right)+S_{\Delta T_{\mathrm{ref}}}^2u^2\left(\Delta T_{\mathrm{ref}}\right)+S_{\Delta P_{\mathrm{ref}}}^2u^2\left(\Delta P_{\mathrm{ref}}\right)+S_\beta^2u^2\left(\beta\right)+S_\kappa^2u^2\left(\kappa\right), \qquad (30)$$

where for convenience, the temperature and pressure differences are given by $\Delta T_{\mathrm{ref}}=T-T_{\mathrm{ref}}$ and $\Delta P_{\mathrm{ref}}=P-P_{\mathrm{ref}}$, respectively. Table 3 lists the values of the sensitivity coefficients and relative standard uncertainties of the sub-measurement variables. Table 3 shows that more than 98 % of the uncertainty is attributed to the reference density. Temperature and pressure measurements have a negligible contribution to the uncertainty in ρ_{MUT} since their respective sensitivity coefficients, $S_{\Delta T_{\mathrm{ref}}}$ and $S_{\Delta P_{\mathrm{ref}}}$, are significantly less than unity. The temperature and pressure sensitivity coefficients are small because β and κ are small. Using Eq. (21), the combined relative standard uncertainty of ρ_{MUT} is 0.004 %. The magnitude of this uncertainty is significant as it contributes more than 11 % to the overall uncertainty in the volume flow measurement (Table 2).

8.3 Combined uncertainty of the LFS mass and volume flow

The uncertainties of sub-measurements are explained in Section 8.2 and their values are itemized in Table 2 and Table 3. In this section we use the results from Section 8.2 to calculate the uncertainties of $\dot{m}_{\mathrm{LFS}}$, and $\dot{Q}_{\mathrm{LFS}}$ as presented in Table 2.

Combined Uncertainty of the LFS Mass Flow

The mass flow measured by the 15 kg/s LFS is calculated using the linear regression formula in Eq. (13). For convenience, we use Eq. (13) with the buoyancy correction, $m_{\mathrm{i}}=W_{\mathrm{i}}/\left[g\left(1-\rho_{\mathrm{air}}/\rho_{\mathrm{water}}\right)\right]$, explicitly included in the formula as given by:

$$\dot{m}_{\mathrm{LFS}}=\left(\frac{N\sum_{i=1}^{N}W_{\mathrm{i}}t_{\mathrm{i}}-\sum_{i=1}^{N}t_{\mathrm{i}}\sum_{i=1}^{N}W_{\mathrm{i}}}{N\sum_{i=1}^{N}t_{\mathrm{i}}^2-\left(\sum_{i=1}^{N}t_{\mathrm{i}}\right)^2}\right)\frac{1}{g\left(1-\rho_{\mathrm{air}}/\rho_{\mathrm{water}}\right)}. \qquad (31)$$

Here, we use the propagation of uncertainty formula given in Eq. (21), which assumes that all correlated uncertainty components are negligible. The uncertainty of each input quantity, the value of its corresponding sensitivity coefficient, and its contribution to the total uncertainty of $\dot{m}_{\mathrm{LFS}}$ is itemized in Table 2. The combined relative standard uncertainty in the LFS mass flow is calculated by:[vii]

$$u^2(\dot{m}_{\mathrm{LFS}})=\sum_{i=1}^{n}S_{t_i}^2u^2(t_{\mathrm{i}})+\sum_{i=1}^{n}S_{W_i}^2u^2(W_{\mathrm{i}})+S_{\dot{m}_{\mathrm{S}}}^2u^2\left(\dot{m}_{\mathrm{S}}\right)+S_{\rho_{\mathrm{water}}}^2u^2(\rho_{\mathrm{water}})+S_{\rho_{\mathrm{air}}}^2u^2(\rho_{\mathrm{air}})+S_{\mathrm{slope}}^2u^2(\mathrm{slope}). \qquad (32)$$

As shown in Table 2, the combined relative standard uncertainty in the LFS mass flow is 0.011 %.

Combined Uncertainty of the Volume Flow at the MUT
The volume flow at the MUT is calculated using Eq. (15). The variables in the expression for volume flow are assumed to be uncorrelated. Applying the RSS approach yields:[vii]

$$u^2\left(\dot{Q}_{\mathrm{LFS}}\right) = S^2_{\dot{m}_{\mathrm{LFS}}} u^2(\dot{m}_{\mathrm{LFS}}) + S^2_{\rho_{\mathrm{MUT}}} u^2(\rho_{\mathrm{MUT}}), \tag{33}$$

where the uncertainty of each input quantity, the value of its corresponding sensitivity coefficient, and its contribution to the total uncertainty in $\dot{Q}_{\mathrm{LFS}}$ is itemized in Table 2. The green shaded box in the table shows that the combined relative standard uncertainty in $\dot{Q}_{\mathrm{LFS}}$ is 0.012 %.

8.4 Combined and expanded uncertainty of the calibration factor

NIST normally uses the LFS to calibrate pulse-generating flow meters, e.g. turbine, positive displacement, or Coriolis flow meters. Coriolis mass flow meters generate a pulse output that is proportional to the mass flow. The meter manufacturer typically has a constant value for the mass per pulse programmed into the meter and, therefore, a mass flow is obtained by multiplying the output frequency by the manufacturer's meter factor. Then a ratio of the mass flow of the LFS to that indicated by the MUT ($\dot{m}_{\mathrm{MUT}}$) is given to the customer for the calibration factor, K_{MUT} :

$$K_{\mathrm{MUT}} = \frac{\dot{m}_{\mathrm{LFS}}}{\dot{m}_{\mathrm{MUT}}}. \tag{34}$$

The NIST calibration can be applied by using a new mass per pulse value, the product of K_{MUT} and the manufacturer's meter factor.

For volume flow meters such as turbine and positive displacement meters, calibration results are often presented using a dimensionless calibration factor called the Strouhal number *St* [5]:

$$St = \frac{f_{\mathrm{MUT}}}{\dot{Q}_{\mathrm{LFS}}}\left(\frac{\pi d^3_{\mathrm{MUT}}}{4}\right), \tag{35}$$

where d_{MUT} is the diameter of the MUT[viii] and f_{MUT} is the frequency reading from the MUT.

Therefore, to determine the uncertainty of a calibration factor for a pulse generating MUT, we determine the sensitivity coefficients for each component by partial differentiation of Eq. (13) or Eq. (15) depending on whether the MUT is a mass flow meter or a volume flow meter, respectively. The uncertainty terms are then combined by RSS to obtain the combined relative uncertainty which in turn, is multiplied by a coverage factor (*k*) determined by the Welch-Satterthwaite method [4, Section G.4] to give the relative expanded uncertainty, $U = k\,u$, at a confidence level of approximately 95 %.

$$U\left(K_{\mathrm{MUT}}\right) = k\,u\left(K_{\mathrm{MUT}}\right) = k\sqrt{\left(S_{f_{\mathrm{MUT}}} u\left(f_{\mathrm{MUT}}\right)\right)^2 + \left(S_{\dot{m}_{\mathrm{LFS}}} u\left(\dot{m}_{\mathrm{LFS}}\right)\right)^2 + \left(2s/\sqrt{N}\right)^2_{\mathrm{BED}}} \tag{36}$$

[viii] Note that the uncertainty in flow meter diameter can be neglected as long as the same reference diameter is used during calibration and usage.

$$U(St) = k\,u(St) = k\sqrt{\left(S_{f_{\mathrm{MUT}}}u(f_{\mathrm{MUT}})\right)^2 + \left(S_{\dot{Q}_{\mathrm{LFS}}}u\left(\dot{Q}_{\mathrm{LFS}}\right)\right)^2 + \left(2s/\sqrt{N}\right)^2_{\mathrm{BED}}} \quad (37)$$

The uncertainty components for a calibration include the relative standard uncertainty of the frequency measurements, $u(f_{\mathrm{MUT}})$, the combined relative standard uncertainty of the volume flow, $u(\dot{Q}_{\mathrm{LFS}})$ or the mass flow, $u(\dot{m}_{\mathrm{LFS}})$, and the reproducibility of the MUT, $s/\sqrt{N}$. Partial differentiation shows that the sensitivity coefficients for frequency $S_{f_{\mathrm{MUT}}}$, volume flow $S_{\dot{Q}_{\mathrm{LFS}}}$, and mass flow $S_{\dot{m}_{\mathrm{LFS}}}$ are 1, -1, and 1, respectively.

The 15 kg/s LFS accepts square wave frequency outputs from the meter under test ranging from 25 Hz to 12,500 Hz. To measure the frequency of the square wave, a data acquisition card measures the period (p) between two successive rising edges using 80 MHz clock pulses. The frequency is calculated by taking the inverse of the period. The clock frequency defines the resolution of the record of start- and stop-time measurements: Δt = 1/80 MHz = 1.25 x 10^{-8} s. The measurements of the meter frequency output are recorded (along with mass and other relevant quantities) in a data record with 0.2 s resolution for subsequent calculations of the average mass flow and frequency by a separate Excel spreadsheet.

Figure 12 illustrates the measurement of the period between two rising edges of the MUT pulses. The start and stop times can each have errors between zero and Δt and there is equal probability for the times in those windows (a rectangular probability distribution). Following the GUM [4] section 4.3.7, the "expected value" for the period is:

$$p = \left[\left(n+1\right)\Delta t - \left(n-1\right)\Delta t\right] / 2 = n\Delta t \quad (38)$$

where n is the number of clock pulses between the meter output rising edges. The associated variance is:

$$u^2(p) = [(n+1)\Delta t - (n-1)\Delta t]^2 / 12 = \Delta t^2 / 3 \quad . \quad (39)$$

Therefore, the standard uncertainty of the period is:

$$u(p) = \Delta t / \sqrt{3} = 0.0125\mu s / \sqrt{3} \quad (40)$$

The worst-case uncertainty occurs at the largest frequency, 12,500 Hz, (shortest period), and it is 0.009 %.

The relative standard uncertainty for mass flow is 0.011 %, and the relative standard uncertainty for the volume flow is 0.012 %. To measure the flow meter reproducibility, the sample standard deviation of ten measurements at flow points that span the range of operation of the LFS was used. Ten measurements were chosen because that is the number of repeat measurements recommended to customers during a NIST calibration. The MUT for the reproducibility evaluation and used as the best existing device (BED) [27] for the meter factor uncertainty was a 5 cm-diameter Coriolis meter. The flow meter irreproducibility was less than 0.010 %

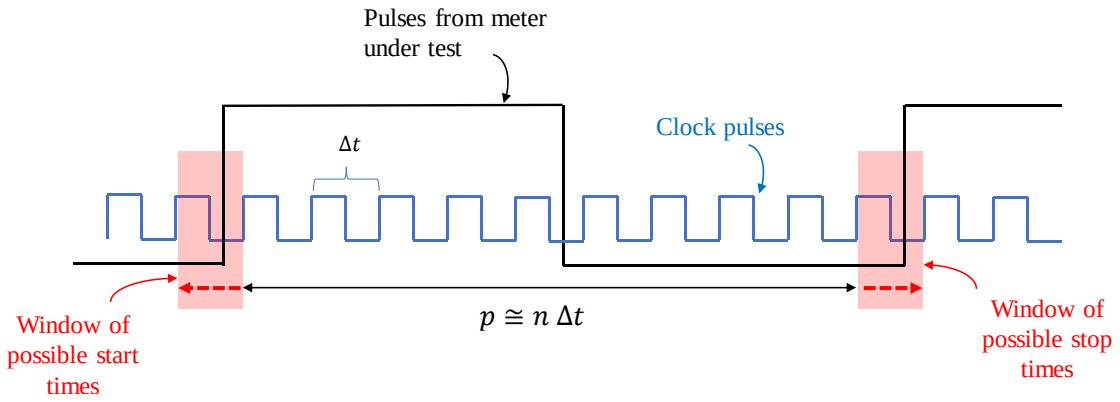

Fig. 12. The frequency of the output from a meter under test is measured using 80 MHz clock pulses. The standard uncertainty of the frequency measurement is related to the period of the clock pulses and a rectangular probability distribution.

Taking into consideration each component of Eq. (13) and Eq. (15) leads to a combined standard uncertainty of 0.017 % and 0.018 % for mass flow and volume flow calibration factors, respectively. Table 4 shows the uncertainty budget for the calibration factors. The effective degrees of freedom (υ_{eff}) that determines the *k* value that gives a 95 % confidence level were determined by the Welch-Satterthwaite Method [4], and is shown for *St* in Eq. (41).

$$\upsilon_{\text{eff}} = \frac{\left(u(St)\right)^4}{\frac{\left(s/\sqrt{N}\right)^4_{\text{BED}}}{10-1} + \frac{\left(S_{Q_{\text{LFS}}} u\left(\dot{Q}_{\text{LFS}}\right)\right)^4}{\infty} + \frac{\left(S_{f_{\text{MUT}}} u\left(f_{\text{MUT}}\right)\right)^4}{\infty}} \tag{41}$$

The effective degrees of freedom for the 15 kg/s LFS is >110000 for the mass and volume calibration factors, which for a 95 % confidence level corresponds to *k* value of 2.0 in both cases. Therefore, the expanded uncertainty for calibration factor determined by the 15 kg/s LFS is 0.035 % and 0.036 % for a mass flow meter and a volume flow meter, respectively.

8.5 Uncertainty considerations for a customer meter under test

The uncertainty analysis reported above is for the 15 kg/s LFS, including the associated connecting volumes and a repeatability component based on the most reproducible device or "check standard" available. The uncertainty analysis for a customer's MUT will depend on the flow meter type and the associated instruments used and therefore the uncertainty for a customer's MUT may be larger than those reported here because the customer's MUT may not be as repeatable[ix] or reproducible[x] as NIST's best existing device.

The NIST calibration report gives the uncertainty of the calibration factor while the meter was at NIST. When the flow meter is used later by the customer, additional uncertainty components must be considered. These include, for example, installation effects, temperature effects, and reproducibility. The MUT's reproducibility, which includes long-term stability, day-to-day performance, and on-off-on stability, can be an order of magnitude larger than the MUT's repeatability. The additional

[ix] Repeatability is defined as the closeness of the agreement between the results of successive measurements of the same measurand carried out under the same conditions of measurement [1].

[x] Reproducibility is defined as the closeness of the agreement between the results of measurements of the same measurand carried out under changed conditions of measurement [1]

uncertainty can be ascertained from multiple calibrations at NIST. Adding that additional uncertainty to that of the NIST calibration will give a more accurate estimate of the MUT's uncertainty when it is used by the customer.

Table 4. Uncertainty budget for the calibration factors (K_{MUT} and *St*). The green highlighted cells correspond to the green highlighted cells in the rightmost column of Table 2.

Variable: Calibration Factor K_{MUT}	**S_{xi} [-]**	**$u(x_i)$ [%]**	**$S_{xi}^2\ u(x_i)^2$**	**Contrib. to $U(K_{MUT})$ [%]**
MUT frequency [Hz]	1	0.009	8.1×10^{-5}	26.84
$\dot{m}_{LFS}$	1	0.011	1.2×10^{-4}	40.01
δBED	1	0.01	1.0×10^{-4}	33.14
			$u\ k = 1$ [%]	**0.017**
			$U\ k = 2$ [%]	**0.035**
Variable: Calibration Factor *St*	**S_{xi} [-]**	**$u(x_i)$ [%]**	**$S_{xi}^2\ u\ (x_i)^2$**	**Contrib. to $U(St)$ [%]**
MUT frequency [Hz]	1	0.009	8.1×10^{-5}	25.49
$\dot{Q}_{LFS}$	-1	0.012	1.4×10^{-4}	43.04
δBED	1	0.01	1.0×10^{-4}	31.47
			$u\ k = 1$ [%]	**0.018**
			$U\ k = 2$ [%]	**0.036**

9.0 Summary

This document describes the 15 kg/s liquid flow calibration system operated by NIST's Fluid Metrology Group to provide flow meter calibrations to customers.

NIST's 15 kg/s LFS is a fully automated, dynamic system that utilizes two PID control loops for flow and pressure stability. The LFS uses only the dynamic method in order to avoid the expense and complexity of a flow diverter. The LFS measures flows from 0.22 kg/s to 15 kg/s with an expanded, 95 % confidence level uncertainty of 0.022% for mass flow and 0.023 % for volume flow in the test section where the MUT is installed. The expanded uncertainty for the meter factor of a unit under test is 0.035 % for a mass flow meter and 0.036 % for a volume flow meter. The uncertainty analysis for the 15 kg/s LFS was validated by comparisons to NIST's existing primary liquid flow standards.

The largest uncertainty of the mass flow measurement comes from the uncertainty of the weigh scale calibration; it accounts for 83 % of the overall uncertainty. The other significant uncertainty component is the slope calculated from the mass-*versus*-time data generated from the weigh scale (Table 2). When converting the mass flow to a volume flow, the density at the MUT becomes a significant contributor to the overall uncertainty (> 11 %).

In this document, we provide an overview of the liquid flow calibration service and the procedures for customers to submit their flow meters to NIST for calibration. We derive the equation for calculating mass and volume flow at the MUT. Finally, we analyze the uncertainty of the flow standards, give supporting data, and provide a sample calibration report in Appendix A.

10.0 References

[1] International Vocabulary of Basic and General Terms in Metrology, 2nd ed. International Organization for Standardization. 1993; Geneva, Switzerland.

[2] Pope, J. G., Johnson, A. N., Filla, B. J., Boyd, J. T., Crowley, C. J., and Bean, V. E. NIST's fully dynamic gravimetric liquid flowmeter standard. Proceedings of the 9th International Symposium on Fluid Flow Measurement. 2015; Arlington, VA.

[3] Mattingly, G.E. Flow measurement proficiency testing. ISA Flow Measurement, 2nd ed. Practical Guides for Measurement and Control, Instrument Society of America. 2001; Ch. 28.

[4] Guide to the expression of uncertainty in measurement. International Organization for Standardization. 1993; Geneva, Switzerland.

[5] Pope, J. G., Wright, J. D., Johnson, A. N., and Moldover, M. R. Extended Lee model for the turbine meter and calibrations with surrogate fluids. Flow Meas. and Instrum. 2012; 24: 71 – 82.

[6] Pope, J. G., Wright, J. D., and Sheckels, S. D. Tests of the extended Lee model using three different turbine meters. Proceedings of the 8th Int. Symp.on Fluid Flow Measurement. 2012; Colorado Springs, CO.

[7] Shinder, I. I. and Moldover, M. R. Feasibility of an accurate dynamic standard for liquid flow. Flow Measurement and Instrumentation. 2010; 21: 128 – 133.

[8] Shinder, I. I. and Moldover, M. R. Dynamic gravimetric standard for liquid flow: model and measurements. Proceedings of the 7th Int. Symp. on Fluid Flow Measurement. 2009; Anchorage, AK.

[9] Shinder, I. I. and Moldover, M. R. Accurately measuring unsteady water flows using a dynamic standard. Proceedings of the Measurement Science Conference. 2009; Anaheim, CA.

[10] Wright, J. D., *Laboratory Primary Standards* in *Flow Measurement: Practical Guides for Measurement and Control*, 2nd edition, D. W. Spitzer editor, The Instrumentation, Systems, and Automation Society, Research Triangle Park, North Carolina, 731- 760. 2001.

[11] A. H. Harvey, S. G. Kaplan, J. H. Burnett. Effect of Dissolved Air on the Density and Refractive Index of Water. International Journal of Thermophysics. 2005; 26: 1495 – 1514.

[12] Ron Benson, Badger Meter Inc., private communication (2008).

[13] Frank M. White, "Fluid Mechanics" (McGraw Hill, New York, 2011).

[14] F.J. Collado, Reynolds transport theorem for a two-phase flow, Applied Physics Letters 90, 024101 (2007).

[15] Coleman, H. W. and Steele, W. G. Experimentation and Uncertainty Analysis for Engineers. 3rd ed. New York: John Wiley and Sons Inc.; 2009.

[16] Lemmon, E. W., Huber, M. L., and McLinden, M. O., "Refprop 23: Reference Fluid Thermodynamic and Transport Properties," NIST Standard Reference Database 23, Version 9,
National Institute of Standards and Technology, Boulder, CO, November, 2010.

[17] Bean, Vern E., Espina, Pedro I., Wright, John D., Houser, John F., Sheckels, Sherry D., and Johnson, Aaron J. NIST Calibration Services for Liquid Volume, National Institute of Standards and Technology (U.S.), Special Publication 250-72. 2009.

[18] Aguilera, J., Rainer, E., and Wendt, G. Dynamic-weighing liquid flow calibration system – Realization of a model based concept. Proc..FLOMEKO. 2007; Johannesburg, South Africa.

[19] Aguilera, J., Rainer, E., and Wendt, G. Dynaimic-weighing liquid flow measurements a description of the measurement process. Proceedings of the 1st International Congress on Mechanical Metrology. 2008; Rio de Janeiro, Brazil.

[20] Tang, K. T. Mathematical Methods for Engineers and Scientists: Fourier analysis, partial differential equations and variational models. Springer. p. 85, 2007.

[21] Chapra, S. C., and Canale, R. P. Numerical Methods for Engineers 6th Ed., McGraw-Hill, New York, NY 2010

[22] Shinder, Iosif I. and Marfenko, Iryna V. NIST Calibration Services for Water Flowmeters. National Institute of Standards and Technology (U.S.), Special Publication 250-73, 2006.

[23] Pope, Jodie G., Wright, John D., Johnson, Aaron N., and Crowley, Christopher J. Liquid Flow Meter Calibrations with the 0.1 L/s and the 2.5 L/s Piston Provers. Nat. Inst. Standards and Technology (U.S.), Special Publication 250-1039r1. 2014.

[24] Taylor, B. N., and Kuyatt, C. E. Guidelines for the evaluating and expressing the uncertainty of NIST measurement results. 1994; NIST TN-1297.

[25] Jaeger, K. B. and Davis, R. S. A Primer for Mass Metrology, National Bureau of Standards (U.S.), Special Publication 700-1, Industrial Measurement Series. 1987: 79. https://nvlpubs.nist.gov/nistpubs/Legacy/SP/nbsspecialpublication700-1.pdf

[26] Patterson, J. B. and Morris, E. C. Measurement of absolute water density, 1 °C to 40 °C. Metrologia. 1994, 31. 277 – 288

[27] Calibration and Measurement Capabilities in the Context of the CIPM MRA, CIPM MRA-D-04 Version 2, September 2010, www.bipm.org/utils/common/CIPM_MRA/CIPM_MRA-D-04.pdf.

Appendix A: Sample Calibration Report

REPORT OF CALIBRATION
FOR
A CORIOLIS LIQUID FLOW METER
January 27, 2021
Coriolis Mass Flow Meter
Flow Range: 5 kg/s to 15 kg/s
Model 678
S/N: 12345

submitted by:
Meter, Inc.
Liquid Drive
Gaithersburg, MD 20899

NIST's 15 kg/s Liquid Flow Standard (LFS) was used to calibrate the meter under test (MUT) [1]. This report presents calibration results for the MUT in tables and figures using the dimensionless calibration factor K_{MUT} as a function of the mass flow, as determined by the primary standard. The calibration factor is:

$$K_{MUT} = \dot{m}_{LFS} / \dot{m}_{MUT} \tag{A1}$$

where $\dot{m}_{MUT}$ is the average output of the MUT during the calibration period, and $\dot{m}_{LFS}$ is the mass flow as determined by the flow standard. The flow from the reference standard and from the MUT were measured over an interval that produced a minimum of 10,000 pulses from the meter under test. The MUT frequency was calculated from the number of pulses divided by the time over which they were collected. The MUT flow was calculated by multiplying the MUT frequency by a customer-specified meter factor (599.9999 pulse/kg). For customers' meters requiring volume flow calibrations, NIST samples the water from the calibration standard and measures its density with a vibrating tube densimeter with uncertainty of 80 parts in 10^6 at the 95 % confidence level. This density data and the temperature of the water in the test section are used to calculate the density of water at the meter under test (ρ_{MUT}) and to convert the mass flow to the volumetric flow through the meter under test. For this calibration, the difference in density from pure water was $\rho_{MUT} - \rho_{water}$ = (0.020±0.006) % and this result was used to compute ρ_{MUT} in Table 1, below.

The MUT installation in the 15 kg/s LFS is shown in Fig. A1. Any extra pipe length upstream from the MUT was of the same nominal diameter as the MUT (5 cm).

[1] Pope, J. G., Johnson, A. N., Filla, Bean, V. E., Moldover, M. R., B. J., Boyd, J. T., Crowley, C. J., and Wright, J. D. Liquid Flow Meter Calibrations with the 15 kg/s Liquid Flow Standard, NIST Special Publication, 2021.

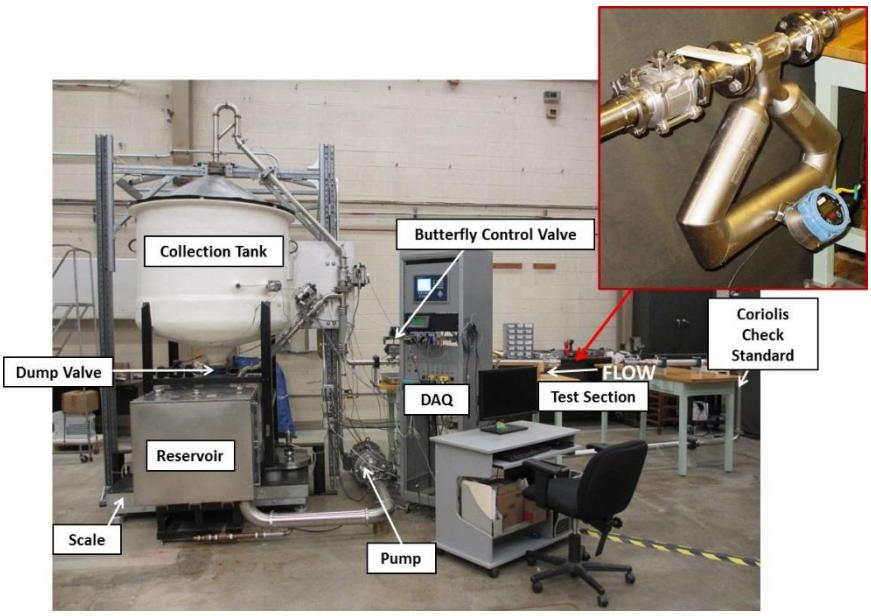

Fig. A1. Photograph of the meter under test SN: 12345 installed in the 15 kg/s LFS.

In order to assess the uncertainty of the calibration factors obtained for the MUT [2, 3], we identified all of the significant uncertainty components and quantified each of them at the 68 % confidence level.

We determined the sensitivity coefficients for each component by partial differentiation of the equations used to calculate the calibration factor. The uncertainty terms were combined by the root-sum-of-squares method (RSS) to obtain the combined relative uncertainty, *u*, which was then multiplied by a coverage factor ($k = 2$) to give the expanded relative uncertainty, $U = k\,u$ at a confidence level of approximately 95 %:

$$U\left(K_{\mathrm{MUT}}\right) = k\,u\left(K_{\mathrm{MUT}}\right) = k\sqrt{\left(s_f u\left(f_{\mathrm{MUT}}\right)\right)^2 + \left(s_{\dot{m}_{\mathrm{LFS}}} u\left(\dot{m}_{\mathrm{LFS}}\right)\right)^2 + \left(2s/\sqrt{N}\right)^2} \qquad \text{(A2)}$$

The uncertainty components for this calibration include the relative standard uncertainty of the frequency measurements, $u(f_{\mathrm{MUT}})$, the combined relative standard uncertainty of the mass flow, $u\left(\dot{m}_{\mathrm{LFS}}\right)$, and the reproducibility of the meter under test, $s/\sqrt{N}$. Partial differentiation of Eq. (A1) yields the sensitivity coefficients for frequency and mass flow: $S_{f_{\mathrm{MUT}}} = \dfrac{\partial K_{\mathrm{MUT}}}{\partial f_{\mathrm{MUT}}} \dfrac{f_{\mathrm{MUT}}}{K_{\mathrm{MUT}}} = 1.0$ and $S_{\dot{m}_{\mathrm{LFS}}} = \dfrac{\partial K_{\mathrm{MUT}}}{\partial \dot{m}_{\mathrm{LFS}}} \dfrac{\dot{m}_{\mathrm{LFS}}}{K_{\mathrm{MUT}}} = -1.0$. The relative standard uncertainty of the frequency measurements is less

[2] Taylor, B. N. and Kuyatt, C. E. Guidelines for Evaluating and Expressing the Uncertainty of NIST Measurement Results. NIST TN1297; 1994.

[3] Coleman, H. W. and Steele, W. G. Experimentation and Uncertainty Analysis for Engineers. New York: John Wiley and Sons; 1989.

than 0.01% and for the 15 kg/s LFS the combined standard mass flow uncertainty is 0.011 % [4].

To measure the flow meter reproducibility, the standard deviation of the mean of 10 measurements was used to calculate the relative standard uncertainty (*i.e.*, the sample standard deviation of the mean divided by the average and expressed as a percentage) at each of the nominal flows. The flow meter reproducibility is a *Type A* uncertainty, while all of the other uncertainty components are *Type B* [5]. Using the uncertainty values given above and Eq. (A2) yield the relative expanded uncertainties for the meter factors listed in the data tables and shown as error bars in the figures.

The calibration and uncertainties presented here are for the calibration factor of the flow meter and are only valid over the range of NIST's calibration of this flow meter. When the flow meter is used by the customer to measure flow, uncertainties beyond the NIST calibration must be considered. These uncertainties include: installation effects, long-term calibration changes, temperature effects on the meter, *etc*.

Table 1. Tabulated results from the 15 kg/s LFS for meter SN:1234.

$\dot{m}_{LFS}$	$\dot{m}_{MUT}$	K_{MUT}	$u(R)$	$U_e\,(k = 2)$	T_{MUT}	[a] ρ_{MUT}
[kg/s]	**[kg/s]**	**[-]**	**[%]**	**[%]**	**[C]**	**[kg/m^3]**
5.0391	5.0398	0.99987	0.002	0.038	23.30	997.47
7.5597	7.5599	0.99998	0.012	0.038	23.22	997.49
10.0797	10.0804	0.99993	0.015	0.042	24.07	997.28
12.5981	12.5978	1.00002	0.016	0.043	23.82	997.34
15.1131	15.1157	0.99983	0.015	0.042	23.24	997.48

[a] For this calibration $\rho_{MUT} - \rho_{water}$ = (0.020±0.006) %

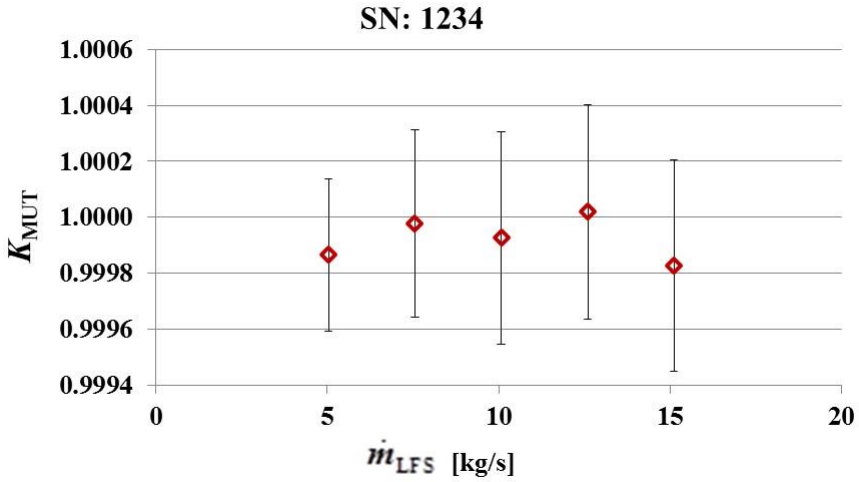

Fig. A2. Calibration results for meter SN:1234.

[4] For the 15 kg/s LFS the relative expanded uncertainty for the mass flow at a meter under test is 0.022 % (k = 2) so that its relative standard uncertainty is 0.011 % (k = 1).

[5] Taylor, B. N. and Kuyatt, C. E. Guidelines for Evaluating and Expressing the Uncertainty of NIST Measurement Results. NIST TN 1297; 1994 edition.

For the Director of the National Institute of Standards and Technology,

Dr. John D. Wright
Group Leader
Fluid Metrology Group
Sensor Science Division
Physical Measurement Laboratory

Dr. Jodie G Pope
Mechanical Engineer,
Fluid Metrology Group
Sensor Science Division
Physical Measurement Laboratory

Calibration performed by:

Joey Boyd
Engineering Technician
Fluid Metrology Group
Sensor Science Division
Physical Measurement Laboratory

Appendix B: Formulas for Sensitivity Coefficient Equations

Table B1. Formulas for Normalized Sensitivity Coefficients

$y = \dot{m}_{\mathrm{LFS}} = \dfrac{N\sum_{i=1}^{N} t_i W_i - \sum_{i=1}^{N} t_i \sum_{i=1}^{N} W_i}{N\sum_{i=1}^{N} t_i^2 - \left(\sum_{i=1}^{N} t_i\right)^2}\left(\dfrac{1}{g\left(1-\rho_{\mathrm{air}}/\rho_{\mathrm{water}}\right)}\right)$	
$\boldsymbol{x_i}$	$S_{x_i} = (\partial y / \partial x_i)(x_i / y)$
W_i	$\dfrac{(t_i - \bar{t})\, m_i}{N\left(\overline{mt} - \bar{t}\,\bar{m}\right)}$
t_i	$\dfrac{t_i\left(m_i - \bar{m}\right) - 2\,\dot{m}_{\mathrm{LFS}}\, t_i\left(t_i - \bar{t}\right)}{N\,\dot{m}_{\mathrm{LFS}}\left(\overline{t^2} - \bar{t}^{\,2}\right)}$
ρ_{air} (EOS)	$\dfrac{\rho_{\mathrm{air}}}{\rho_{\mathrm{water}} - \rho_{\mathrm{air}}}$
ρ_{water}	$\dfrac{-\rho_{\mathrm{air}}}{\rho_{\mathrm{water}} - \rho_{\mathrm{air}}}$
Slope (Linear Regression)	Unity
$y = \dot{m}_{\mathrm{CV}} = \dfrac{\rho_{\mathrm{ref}}\left[\beta\left(\Delta T_{\mathrm{fi}}\right) + \kappa\left(\Delta P_{\mathrm{fi}}\right)\right] V_{\mathrm{CV}}}{N \cdot \tau}$	
$\boldsymbol{x_i}$	$S_{x_i} = (\partial y / \partial x_i)(x_i / y)$
ρ_{ref}	Unity
β	$\dfrac{\beta\,\Delta T_{\mathrm{if}}}{\left(\beta\,\Delta T_{\mathrm{if}} + \kappa\,\Delta P_{\mathrm{fi}}\right)}$
ΔT_{fi}	$\dfrac{\beta\,\Delta T_{\mathrm{if}}}{\left(\beta\,\Delta T_{\mathrm{if}} + \kappa\,\Delta P_{\mathrm{fi}}\right)}$
κ	$\dfrac{\kappa\,\Delta P_{\mathrm{fi}}}{\left(\beta\,\Delta T_{\mathrm{if}} + \kappa\,\Delta P_{\mathrm{fi}}\right)}$
ΔP_{fi}	$\dfrac{\kappa\,\Delta P_{\mathrm{fi}}}{\left(\beta\,\Delta T_{\mathrm{if}} + \kappa\,\Delta P_{\mathrm{fi}}\right)}$
V_{c}	Unity
$N\,\tau$	$1/N$
$y = \rho_{\mathrm{MUT}} = \rho_{\mathrm{ref}}\left[1 - \beta\left(\Delta T_{\mathrm{ref}}\right) + \kappa\left(\Delta P_{\mathrm{ref}}\right)\right]$	
$\boldsymbol{x_i}$	$S_{xi} = (\partial y / \partial x_i)(x_i / y)$
ρ_{ref}	Unity
β	$\dfrac{\beta\,\Delta T_{\mathrm{ref}}}{\left(1 - \beta\,\Delta T_{\mathrm{ref}} + \kappa\,\Delta P_{\mathrm{ref}}\right)}$
ΔT_{ref}	$\dfrac{\beta\,\Delta T_{\mathrm{ref}}}{\left(1 - \beta\,\Delta T_{\mathrm{ref}} + \kappa\,\Delta P_{\mathrm{ref}}\right)}$

Table B1. Formulas for Normalized Sensitivity Coefficients

κ	$\frac{\kappa \Delta P_{\text{ref}}}{\left(1-\beta \Delta T_{\text{ref}}+\kappa \Delta P_{\text{ref}}\right)}$
ΔP_{ref}	$\frac{\kappa \Delta P_{\text{ref}}}{\left(1-\beta \Delta T_{\text{ref}}+\kappa \Delta P_{\text{ref}}\right)}$
$y=\dot{Q}_{\text{LFS}}=\dot{m}_{\text{LFS}}/\rho_{\text{MUT}}$	
x_i	$S_{xi}=\left(\partial y/\partial x_i\right)\left(x_i/y\right)$
$\dot{m}_{\text{LFS}}$	Unity
ρ_{MUT}	Unity

Notes: 1) Variables with bars over them indicate average values over a collection period.

2) NOTE that $\frac{\partial \dot{m}_{\text{LFS}}}{\partial \Delta T_{\text{ref}}}=\frac{\partial \dot{m}_{\text{LFS}}}{\partial (T_{\text{water}}-T_{\text{ref}})}=\frac{\partial \dot{m}_{\text{LFS}}}{\partial T_{\text{water}}}$ because T_{ref} is a constant. That is, the partial derivative of the mass flow with respect to the difference in temperature is the same as the derivative with respect to the temperature alone. Moreover, since the value of T_{ref} is defined, it has no uncertainty. The same is true for ΔP_{ref} .

Appendix C: Nomenclature

Variable	Description
a_1, a_2	Polynomial coefficients
β	Volumetric thermal expansion coefficient
c	Intercept of mass vs. time plot
d_{MUT}	Inside diameter of meter under test
E_n	Normalized degree of equivalence
f_{MUT}	Frequency output by meter under test
g	Acceleration due to gravity, 9.8 m/s^2
h	Height of water in collection tank
k	Coverage factor
K_{MUT}	Meter factor, $\dot{m}_{LFS} / \dot{m}_{MUT}$
κ	Isothermal compressibility factor
m	Mass
m_a	Apparent mass
m_{Cal}	Calibrated mass from the weigh scale reading.
$\dot{m}$	Mass flow
$\dot{m}_{run}$	Running average mass flow
$\dot{m}_{LFS}$	Mass flow measured by the liquid flow standard
$\dot{m}_S$	Mass flow due to storage effects in the connecting volume
$\dot{m}_{MUT}$	Mass flow measured by the meter under test
$\dot{m}_{scale}$	Mass flow determined from buoyancy-corrected weigh scale readings
$\langle \dot{m}_{t1,t2} \rangle$	Mass flow into weigh tank averaged over time interval $t_2 - t_1$
N	Number of data points
P	Pressure
$\dot{p}$	Vertical rate of momentum transfer, or impulse
$\dot{Q}_{LFS}$	Volume Flow measured by the liquid flow standard
r	Correlation coefficient
RH	Relative Humidity
ρ	Density

Variable	Description
s	Standard deviation of a sample of N values
S	Normalized sensitivity coefficient
St	Strouhal number
t	Time
T	Temperature
τ	Period of mass measurements = 209.718 ms
u	Relative standard uncertainty, or 68 % confidence level
U	Relative expanded uncertainty, or 95 % confidence level
$\vec{v}$	Velocity
V_S	Volume of the connecting volume between the MUT and the collection tank
W	Force applied to the weigh scale
W_{tare}	Force of the unfilled collection tank on the weigh scale
x	General input variable
y	General output variable